

Contract No. W-7405-eng-26

Neutron Physics Division

NEUTRON AND SECONDARY-GAMMA-RAY TRANSPORT CALCULATIONS FOR
14-MeV AND FISSION NEUTRON SOURCES IN AIR-OVER-GROUND
AND AIR-OVER-SEAWATER GEOMETRIES

J. V. Pace, III,* D. E. Bartine,
and F. R. Mynatt

NOTE:

Work supported by
DEFENSE NUCLEAR AGENCY
under
Subtask PE 074

AUGUST 1975

*Computer Sciences Division.

NOTICE

This report was prepared as an account of work sponsored by the United States Government. Neither the United States nor the United States Energy Research and Development Administration, nor any of their employees, nor any of their contractors, subcontractors, or their employees, makes any warranty, express or implied, or assumes any legal liability or responsibility for the accuracy, completeness or usefulness of any information, apparatus, product or process disclosed, or represents that its use would not infringe privately owned rights.

OAK RIDGE NATIONAL LABORATORY
Oak Ridge, Tennessee 37830
operated by
UNION CARBIDE CORPORATION
for the

U.S. ENERGY RESEARCH AND DEVELOPMENT ADMINISTRATION

DISTRIBUTION OF THIS DOCUMENT UNLIMITED



4

7

2

4

2

2

2

2



DISCLAIMER

This report was prepared as an account of work sponsored by an agency of the United States Government. Neither the United States Government nor any agency Thereof, nor any of their employees, makes any warranty, express or implied, or assumes any legal liability or responsibility for the accuracy, completeness, or usefulness of any information, apparatus, product, or process disclosed, or represents that its use would not infringe privately owned rights. Reference herein to any specific commercial product, process, or service by trade name, trademark, manufacturer, or otherwise does not necessarily constitute or imply its endorsement, recommendation, or favoring by the United States Government or any agency thereof. The views and opinions of authors expressed herein do not necessarily state or reflect those of the United States Government or any agency thereof.

DISCLAIMER

Portions of this document may be illegible in electronic image products. Images are produced from the best available original document.

TABLE OF CONTENTS

	<u>Page</u>
Abstract	v
Introduction	1
Problem Description	1
Results	5
Conclusions	10
References	15
Appendix	16

fec



1

2

3

4

5

6

7

8



Abstract

Radiation transport calculations have been performed with the DOT-III code for a 14-MeV neutron source and a tactical weapon fission neutron source in air-over-ground and air-over-seawater geometries. The source heights were 1, 50, 100, 200, and 300 m for the air-over-ground calculations and 50 m for the air-over-seawater calculations. The results were obtained as neutron and secondary-gamma-ray fluxes throughout a cylindrical system having a height of approximately 1300 m and a radius of about 1500 m, the lower 50 cm of the cylinder being either ground or seawater. Several ionization and tissue-dose response functions were applied to the fluxes obtained for positions on the interfaces. The air-over-ground results indicate that an optimal source height can be specified for the maximum neutron dose at a given ground range. They also show the source height and ground-range combinations for which the air-over-ground neutron and gamma-ray tissue doses are greater than those at equivalent ranges in infinite air.



.

.

.

.

.



Introduction

During the past seven or eight years -- since the advent of multigroup transport computer codes that can handle neutron and gamma-ray interactions simultaneously -- several calculations have been performed to predict the neutron and secondary-gamma-ray fields produced by the detonation of nuclear weapons at various heights above the ground.¹⁻⁴ The neutron sources used for the calculations have included a fission source, a thermonuclear source, and monoenergetic sources with energies up to 14 MeV.

Calculations of this type yield sets of data that are too massive for publication and are usually stored on magnetic tape. In an attempt to aid the users of such data, the Defense Nuclear Agency (DNA) sponsored the development at Science Applications, Inc. of a computer code (called the ATR code⁵) that constructs radiation environments for specified weapons from the data sets. Since all the transport data available to ATR were obtained with cross sections that predated the latest ENDF/B-IV release, DNA requested that ORNL provide an updated data base by performing a new set of air-over-ground calculations for two sources -- a tactical weapon fission source and a 14-MeV source. At the same time, DNA requested that ORNL also perform similar calculations for an air-over-seawater geometry in order to compare the relative effects of ground and seawater on the radiation environments.

This report describes the calculations and discusses those results obtained for positions on the air-ground and air-seawater interfaces for several source heights.

Problem Description

The air-over-ground and air-over-seawater problems were calculated with the DOT-III discrete ordinates code⁶ in two-dimensional cylindrical geometry using an S_8 (48-angle) angular quadrature. In each case the cylinder height was ~ 1300 m and its radius was 1490 m. The ground (or seawater) was treated as a 50-cm thickness at the bottom of the cylinder,

and the air was assumed to comprise the remainder of the system. The sources were placed on the cylinder axis at various heights above the ground (or seawater), and the neutron and gamma-ray fluxes were calculated for "all points" in the surrounding medium. However, due to the need for a reflective air mass beyond the points of interest, the results are considered to be accurate only for heights less than 1000 m and for radii (ground ranges) less than 1200 m. The overall geometry of the problem is shown in Fig. 1.

The elemental compositions assumed for the ground, seawater, and air are given in Table 1, along with the corresponding MAT and MOD numbers of the cross sections used from the ENDF/B-IV files. The ENDF/B point data were processed into the required multigroup structure by the AMPX code.⁷

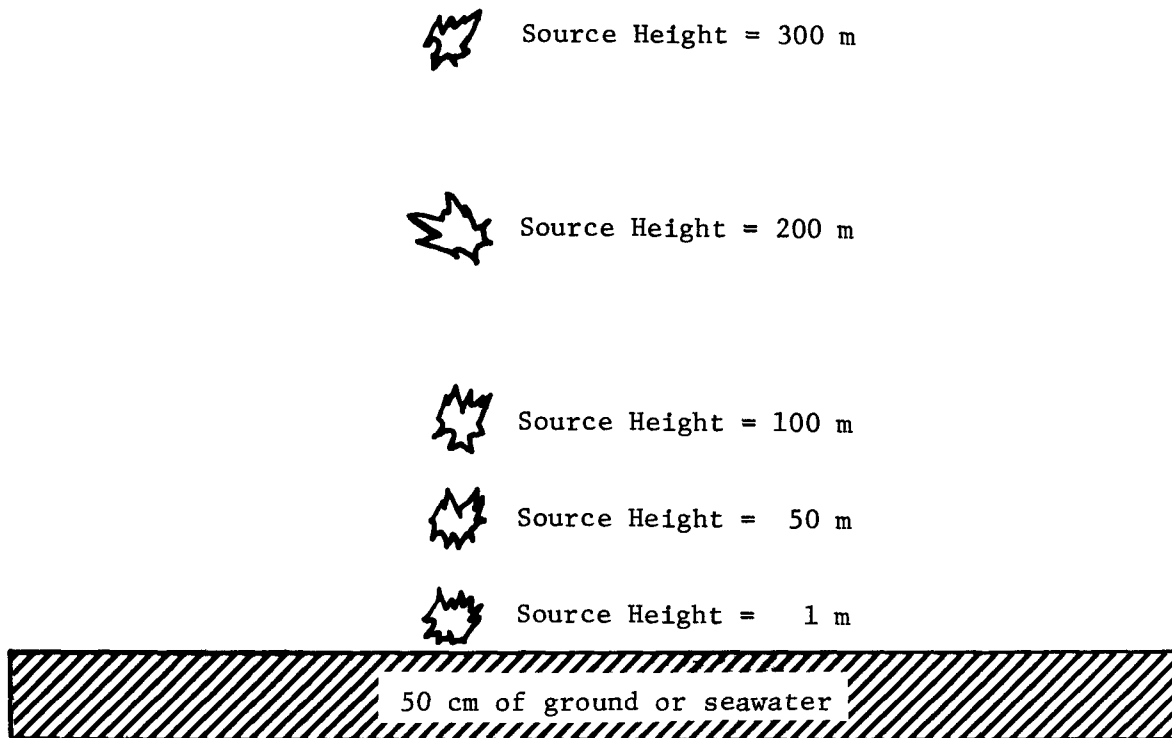


Fig. 1. Schematic of Air-Over-Ground and Air-Over-Seawater Geometries. The system's height and radius were 1295.5 m and 1490 m, respectively. The detectors were 0.5 m above the interface.

Table 1. Material Compositions and Cross Sections
Used in Calculations

Element	Cross Sections ^a		Composition (atoms/b-cm)		
	Mat No.	Mod. No.	Air ($\rho=1.22$ g/l)	Ground ($\rho=1.7$ g/cc)	Seawater ($\rho=1.025$ g/cc)
H	4148	2		9.7656-3	6.64-2
N	4133	4	4.0242-5 ^a		
O	4134	2	1.0697-5	3.4790-2	3.32-2
Na	4156	0			2.81-4
Mg	4512	0			3.00-5
Al	4135	3		4.8828-3	
Si	4151	2		1.1597-2	
Cl	1149	-			3.30-4

^aRead: 4.0242×10^{-5} .

They were first put into a structure consisting of 105 neutron groups and 18 gamma-ray groups, after which the neutron cross sections were collapsed into 22 groups. All the cross sections were then 14-MeV flux-weighted via one-dimensional ANISN⁸ calculations for the air-over-ground and air-over-seawater environments. The angular dependence of scattering was approximated by a P_3 Legendre polynomial series for both neutrons and gamma rays.

As pointed out above, the two sources used for the calculations were a 14-MeV neutron source and a tactical weapon fission source. The fission source, originally described by seven energy groups between 0.0033 MeV and 10 MeV, was expanded to the 12 groups included for this energy region in the 22-group structure (see Table 2). The source heights were 1, 50, 100, 200, and 300 m for the air-over-ground problems and 50 m for the air-over-seawater problems.

The sources were represented in the calculations as point sources, which in the past has introduced ray effects. However, the DOT-III code has a special option available with which the point source can be

Table 2. Energy Spectrum of Tactical Weapon
Fission Neutron Source

Group	Upper Energy (MeV)	Fraction per Energy Group
1	17	0.0
2	12.2	0.0
3	10	$7.342 \cdot 10^{-3}$ ^a
4	8.18	$1.274 \cdot 10^{-2}$
5	6.36	$1.832 \cdot 10^{-2}$
6	4.96	$1.177 \cdot 10^{-2}$
7	4.06	$5.481 \cdot 10^{-2}$
8	3.01	$2.871 \cdot 10^{-2}$
9	2.46	$5.743 \cdot 10^{-3}$
10	2.35	$1.060 \cdot 10^{-1}$
11	1.83	$1.468 \cdot 10^{-1}$
12	1.11	$2.159 \cdot 10^{-1}$
13	0.55	$1.693 \cdot 10^{-1}$
14	0.111	$2.227 \cdot 10^{-1}$
15-22	0.00335 ^b	0.0

^aRead: 7.342×10^{-3} .

^bLower energy limit is 1.1-11.

distributed over the entire system as a first-collision source. DOT-III then calculates the collided flux, adding it to the uncollided flux at problem termination.

Another difficulty in the calculations was overcome through the use of a weighted diamond difference option in DOT-III. In a preliminary set of calculations use of the linear step option for flux transport across a single interval resulted in a radial flux distribution which exhibited step-function type changes at certain spatial positions. But when the weighted diamond difference option was used, the calculation converged to a smooth flux distribution in a shorter time.

Results

Several response functions were applied to the neutron and gamma-ray fluxes calculated for positions on the interfaces, and it is these results that are presented in this report. Scalar flux tapes for the entire series of calculations are available from the ORNL Radiation Shielding Information Center.

The response functions applied to the neutron interface fluxes were neutron ionization response functions, Henderson tissue dose response functions,⁹ and Auxier-Snyder tissue dose response functions.¹⁰ Those applied to the gamma-ray fluxes were gamma-ray ionization response functions, Henderson tissue dose response functions,⁹ and Claiborne-Trubey tissue dose response functions.¹¹ These response functions are listed in Tables 3 and 4 for neutrons and gamma rays respectively. Plots of the resulting ionizations and tissue doses were obtained for each source at each source height and are included as an appendix to this report. All the results are normalized to one source neutron since both sources were normalized to 1.0.

Study of the neutron dose plots from the air-over-ground calculations indicates that an optimal relationship exists between the source height and the ground range. That is, a burst height may be specified which will give the maximum dose for a given ground range. This is illustrated in Fig. 2, in which the Henderson tissue dose is plotted as a function of the height of the 14-MeV source for several ground ranges. (This figure is designed to show the relative shapes of the curves for the four ground ranges. Absolute values of the dose are to be read from Table 5.) Figure 2 shows that as the ground range increases, the source height that yields the largest calculated dose also increases. Although an adjoint calculation would be required to identify the exact optimal source height for a specific ground range, Fig. 2 clearly demonstrates the existence of an optimal source height. Similar observations may be made concerning the results of the air-over-ground calculations performed with a weapon fission source.

Table 3. Neutron Response Functions

Group	Upper Energy (MeV)	Neutron Ionization [(rad-Si)/(n/cm ²)]	Henderson Tissue Dose [rads/(n/cm ²)]	Auxier-Snyder Tissue Dose [rads/(n/cm ²)]
1	1.700+1 ^a	8.60-10	5.46-9	7.61-9
2	1.221+1	9.90-10	5.13-9	6.68-9
3	1.000+1	8.10-10	4.84-9	6.16-9
4	8.187+0	5.50-10	4.61-9	5.87-9
5	6.360+0	1.60-10	4.44-9	5.56-9
6	4.966+0	9.00-11	4.13-9	5.15-9
7	4.066+0	5.40-11	4.01-9	4.55-9
8	3.012+0	3.60-11	3.39-9	4.03-9
9	2.466+0	3.00-11	3.15-9	3.83-9
10	2.350+0	2.70-11	3.09-9	3.74-9
11	1.827+0	2.10-11	2.64-9	3.52-9
12	1.108+0	1.70-11	1.97-9	2.92-9
13	5.502-1	1.40-11	1.12-9	1.47-9
14	1.111-1	0.0	2.29-10	5.21-10
15	3.355-3	0.0	0.0	4.95-10
16	5.829-4	0.0	0.0	5.57-10
17	1.013-4	0.0	0.0	5.96-10
18	2.902-5	0.0	0.0	6.21-10
19	1.068-5	0.0	0.0	6.34-10
20	3.059-6	0.0	0.0	6.30-10
21	1.126-6	0.0	0.0	6.07-10
22	4.140-11 ^b	0.0	0.0	5.31-10

^aRead: 1.700 x 10¹.

^bLower limit is 1.000-11.

Table 4. Gamma-Ray Response Functions

Group	Upper Energy (MeV)	Gamma-Ray Ionization [(rad-Si)/(γ/cm ²)]	Henderson Tissue Dose [rad/(γ/cm ²)]	Claiborne-Trubey Tissue Dose [rad/(γ/cm ²)]
1	1.20+1 ^a	2.80-9	2.42-9	2.43-9
2	8.00+0	2.28-9	2.07-9	2.07-9
3	6.50+0	1.83-9	1.76-9	1.76-9
4	5.00+0	1.48-9	1.59-9	1.50-9
5	4.00+0	1.20-9	1.27-9	1.27-9
6	3.00+0	9.85-10	1.08-9	1.09-9
7	2.50+0	8.40-10	8.75-10	9.58-10
8	2.00+0	7.12-10	7.35-10	8.37-10
9	1.66+0	6.10-10	6.44-10	7.29-10
10	1.33+0	5.05-10	5.30-10	6.09-10
11	1.00+0	4.10-10	4.45-10	5.03-10
12	8.00-1	3.28-10	3.50-10	4.17-10
13	6.00-1	2.37-10	2.56-10	3.22-10
14	4.00-1	1.65-10	1.77-10	2.32-10
15	3.00-1	1.17-10	1.22-10	1.77-10
16	2.00-1	7.25-11	6.60-11	1.20-10
17	1.00-1	9.75-11	3.90-11	7.47-11
18	5.00-2 ^b	4.13-10	8.37-11	1.47-10

^aRead: 1.20 x 10¹.^bLower limit is 2.00-2.

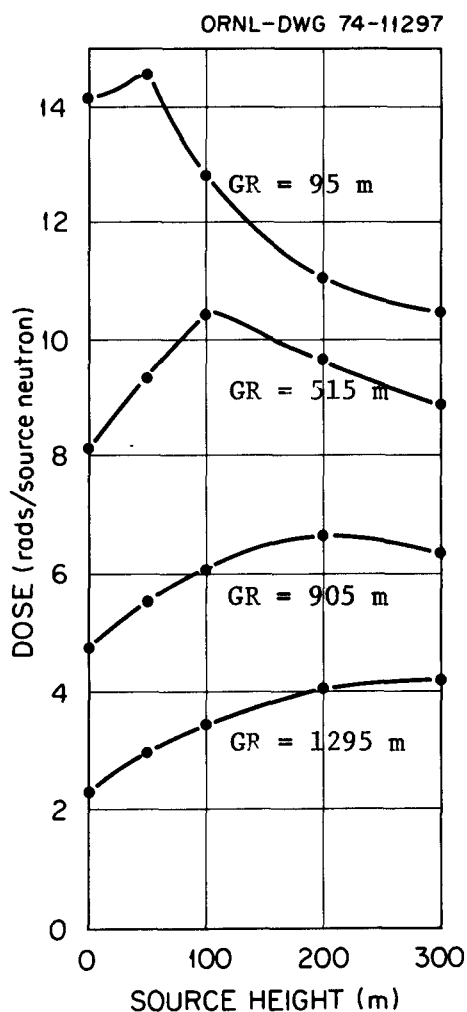


Fig. 2. Plot Showing Relative Shapes of Henderson Neutron Tissue Doses at Various Ground Ranges (GR) from a 14-MeV Source at Various Heights. See Table 5 for exact values of doses.

The air-over-ground plots also show the effect of the ground on the dose. Earlier investigators^{1,3} have reported that the presence of the ground enhances the dose at short slant ranges but depresses the dose at large slant ranges, compared to the dose at the same position obtained from an infinite-air calculation. Figure 3 indicates the ground ranges for which ground enhances the neutron and gamma-ray doses (area to the left of the lines) as a function of source height for the 14-MeV source. The regions to the right of the lines therefore represent 14-MeV burst height and ground range combinations for which an infinite-air

Table 5. Henderson Neutron Doses Produced by a 14-MeV Source in an Air-Over-Ground Geometry

Ground Range ^a (m)	Dose (rads/source neutron) at Source Height of				
	1 m	50 m	100 m	200 m	300 m
95	4.14-18 ^b	4.56-18	2.80-18	1.01-18	4.42-19
515	4.11-20	5.35-20	6.40-20	5.67-20	4.84-20
905	2.76-21	3.53-21	4.05-21	4.67-21	4.33-21
1295	2.31-22	2.97-22	3.41-22	4.01-22	4.17-22

^aDetector is 0.5 m above the ground.

^bRead: 4.14×10^{-18} rads/source neutron.

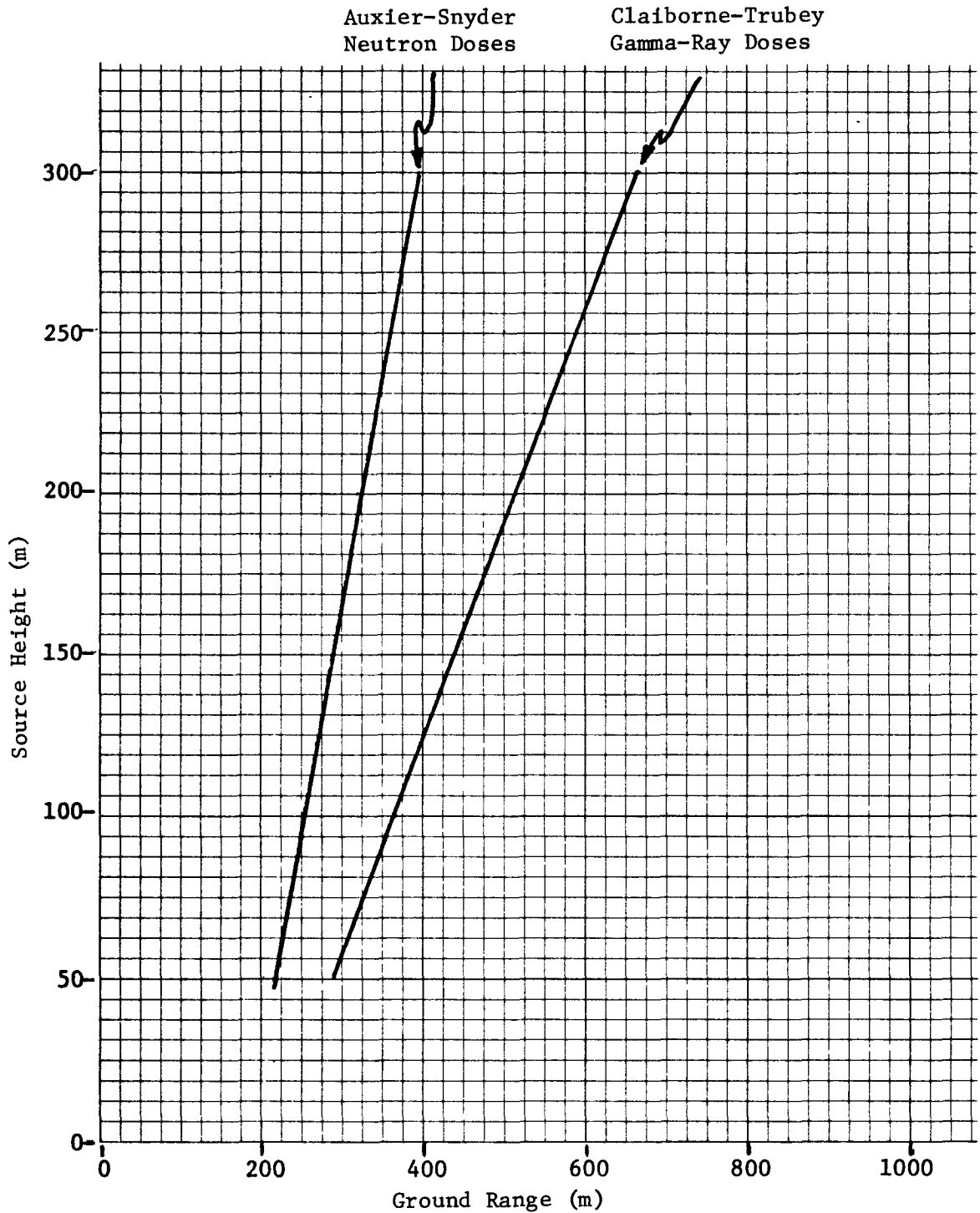


Fig. 3. Plots of 14-MeV Source Height and Approximate Ground Range Combinations for Which the Air-Over-Ground Neutron and Secondary-Gamma-Ray Interface Doses Are Equivalent to Infinite-Air Doses. For combinations to the right of the lines the infinite-air calculations yield higher doses, and for combinations to the left of the lines the air-over-ground calculations yield higher doses.

calculation is conservative. Figure 4 shows similar plots for the neutron and gamma-ray doses produced by the weapon fission source, and Fig. 5 shows similar plots for the total tissue doses produced by both sources.

The air-over-seawater calculations (50-m source height) showed that the neutron dose at the interface was depressed while the gamma-ray dose was enhanced relative to the air-over-ground results. Table 6 shows comparative doses at the interface for air-over-ground (A/G) and air-over-seawater (A/SW) calculations at three ground ranges for the 14-MeV and weapon fission sources, respectively. Note that the total dose is dominated by the neutron dose and is therefore depressed for A/SW relative to A/G. Figure 6 shows the calculated gamma-ray dose due to a weapon fission source as a function of ground range along the air-ground and air-sea interfaces.

Analysis of the results showed that the seawater both reduced the neutron flux and softened the neutron spectrum to a greater extent than the ground did, thereby reducing the neutron dose but increasing the gamma-ray dose due to increased capture-gamma-ray production. In a detailed investigation of the gamma-ray production involved, one-dimensional spherical ANISN⁸ calculations were performed for the fission source in the air-over-seawater configuration with and without chlorine and also for the air-over-ground configuration. The results are given in Table 7 as a function of gamma-ray energy. The thermal (n, γ) reaction for chlorine produces gamma rays with energies primarily from 6 to 8 MeV, while hydrogen produces only a 2.2-MeV gamma ray. As Table 7 indicates, the chlorine and hydrogen captures contribute substantially to the gamma-ray dose at the interface, but the presence of chlorine has a dominant effect, although it is only a trace element, as indicated by the number densities given in Table 1.

Conclusions

The air-over-ground calculations demonstrate the existence of an optimal height of burst for a specific ground range. They also delineate the conditions under which air-over-ground calculations are conservative

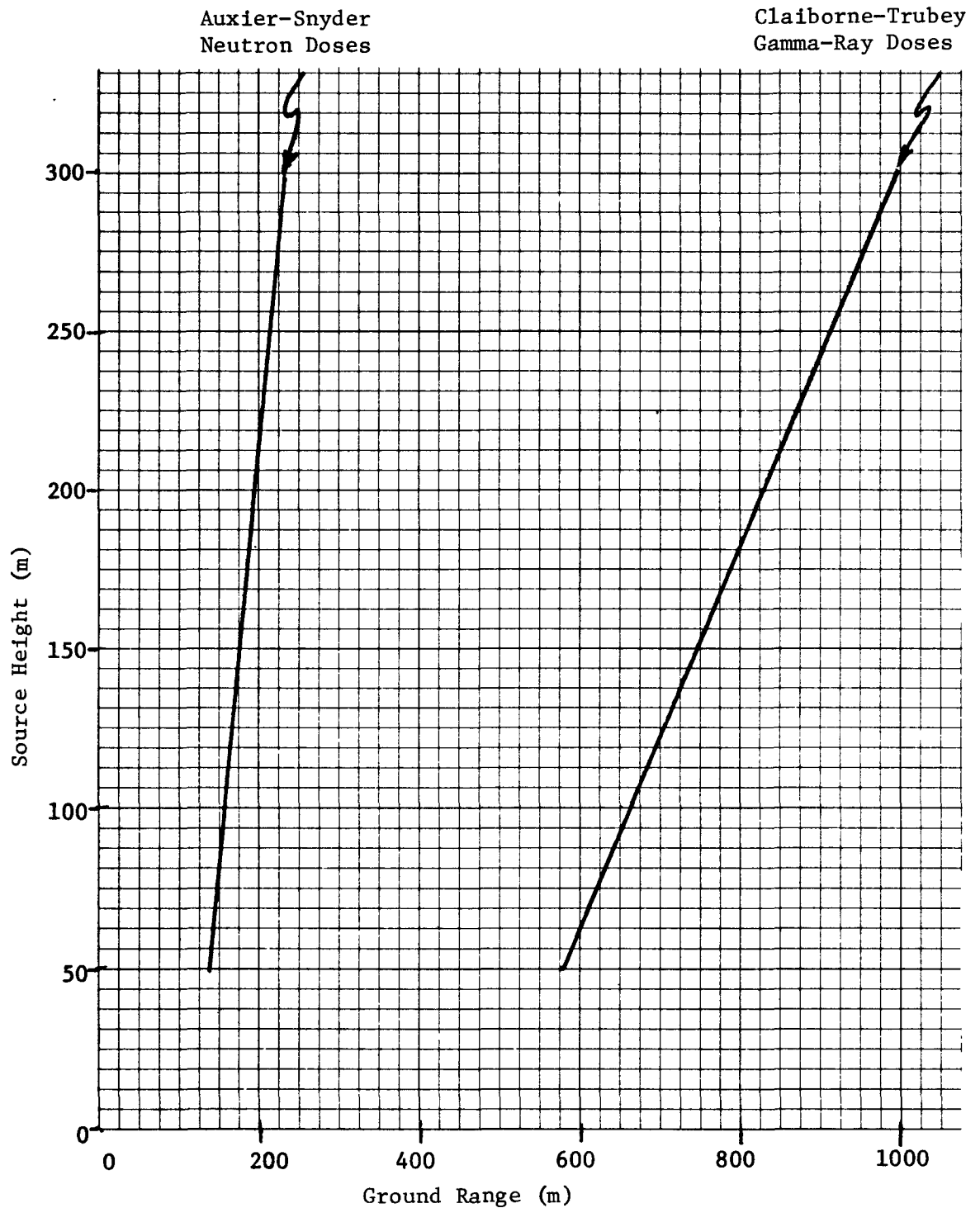


Fig. 4. Plots of Weapon Fission Source Height and Approximate Ground Range Combinations for Which the Air-Over-Ground Neutron and Secondary-Gamma-Ray Interface Doses Are Equivalent to Infinite-Air Doses. For combinations to the right of the lines the infinite-air calculations yield higher doses, and for combinations to the left of the lines the air-over-ground calculations yield higher doses.

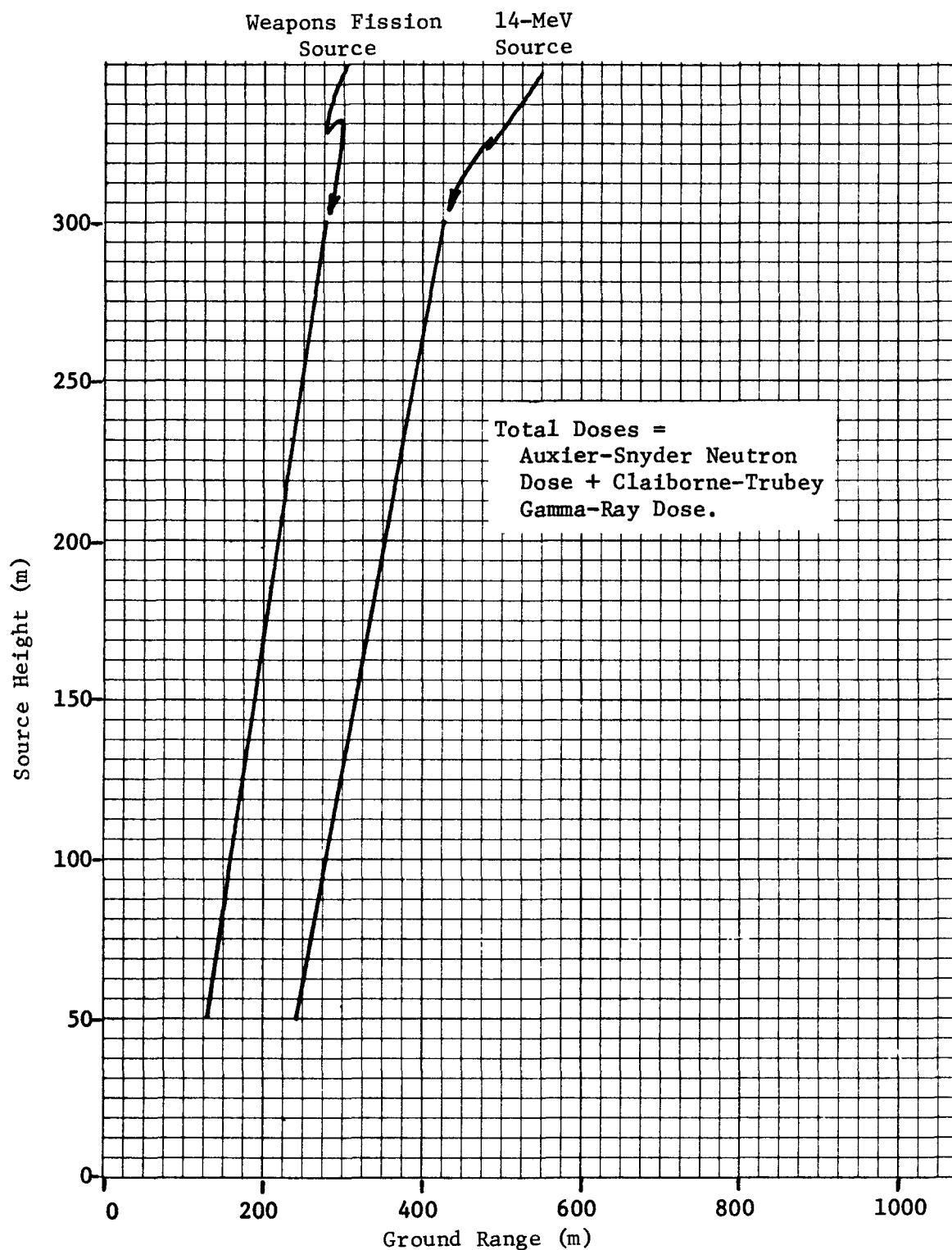


Fig. 5. Plots of Source Height and Approximate Ground Range Combinations for Which the Air-Over-Ground Total Interface Doses Produced by a 14-MeV Source and a Weapons Fission Source Are Equivalent to Infinite-Air Doses. For combinations to the right of the lines the infinite-air calculations yield higher doses, and for combinations to the left of the lines the air-over-ground calculations yield higher doses.

Table 6. Henderson Neutron and Gamma-Ray Tissue Doses 0.5 m Above Air-Over-Ground (A/G) and Air-Over-Seawater (A/SW) Interface (Burst height = 50 m)

Ground Range (m)	Neutron Dose (rads)			Gamma-Ray Dose (rads)			Total Dose (rads)		
	A/G	A/SW	$\Delta\%$ ^a	A/G	A/SW	$\Delta\%$	A/G	A/SW	$\Delta\%$
<u>Fission Source</u>									
0	1.14-17 ^b	8.47-18	-26	6.41-19	2.00-18	212	1.20-17	1.05-17	-13
515	1.73-20	1.14-20	-34	2.69-21	4.35-21	62	2.00-20	1.58-20	-21
995	3.50-22	2.29-22	-35	1.28-22	1.70-22	33	4.78-22	3.99-22	-16
<u>14-MeV Source</u>									
0	2.51-17	2.14-17	-15	2.67-18	2.90-18	9	2.78-17	2.43-17	-13
515	5.35-20	4.27-20	-20	1.09-20	1.21-20	11	6.44-20	5.48-20	-15
995	1.98-21	1.48-21	-25	6.73-22	7.46-22	11	2.65-21	2.23-21	-16

$$^a \Delta\% = \frac{A/SW - A/G}{A/G} \times 100\%.$$

$$^b \text{Read: } 1.14 \times 10^{-17}.$$

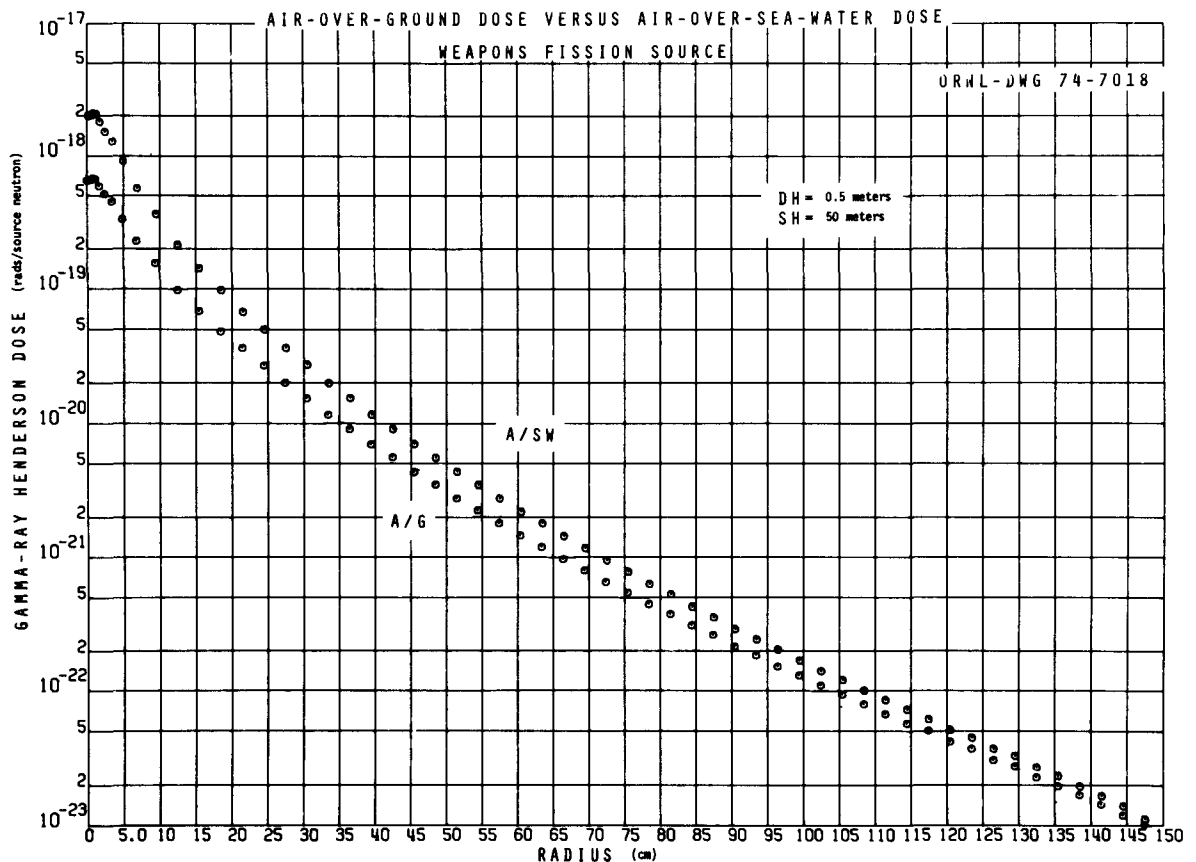


Fig. 6. Henderson Gamma-Ray Tissue Doses at the Air-Ground and Air-Seawater Interfaces for the Weapon Fission Source.

Table 7. Henderson Gamma-Ray Tissue Doses 0.5 m Above
Air-Over-Ground and Air-Over-Seawater Interfaces,
With and Without Chlorine in Seawater
(Fission Source at Height of 50 m)

Energy Range (MeV)	A/G Dose (rads)	A/SW Dose (rads)	$\Delta\%$ ^a for A/SW	A/SW Dose (w/o Cl) (rads)	$\Delta\%$ for A/SW w/o Cl
2.5-12.0	1.45-10 ^b	2.32-10	+ 60	5.08-11	- 65
2.0-2.5	3.61-11	1.64-10	+354	2.02-10	+460
0.02-2.0	6.75-11	1.42-10	+111	1.04-10	+ 54
0.02-12.0	2.49-10	5.38-10	+116	3.56-10	+ 43

^a $\Delta\% = \frac{A/SW - A/G}{A/G} \times 100\%.$

^bRead: $1.45 \times 10^{-10}.$

with respect to infinite-air calculations for the sources and span of ground ranges considered here.

The air-over-seawater results indicate that compared to air-over-ground results, the neutron dose is lower and the gamma-ray dose is higher. Also, the presence of the trace element chlorine in seawater has a strong effect on the gamma-ray dose due to the production of capture gamma rays in the 6- to 8-MeV range.

Finally, this study indicated that the weighted diamond difference option in DOT-III is more satisfactory for air-over-ground calculations than the linear-step option used in previous calculations.

References

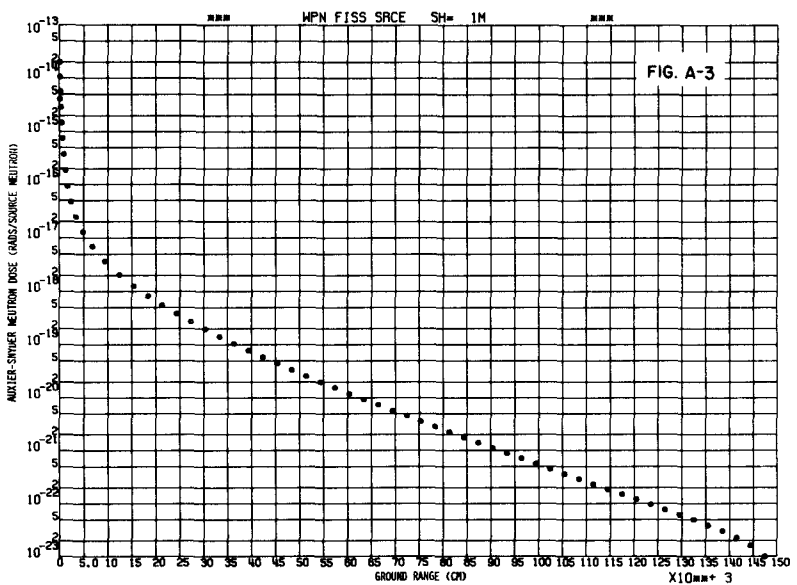
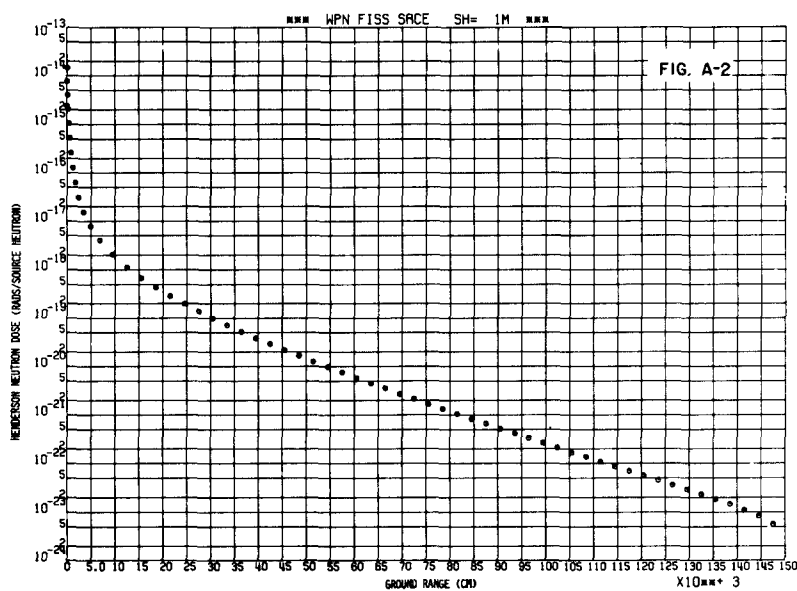
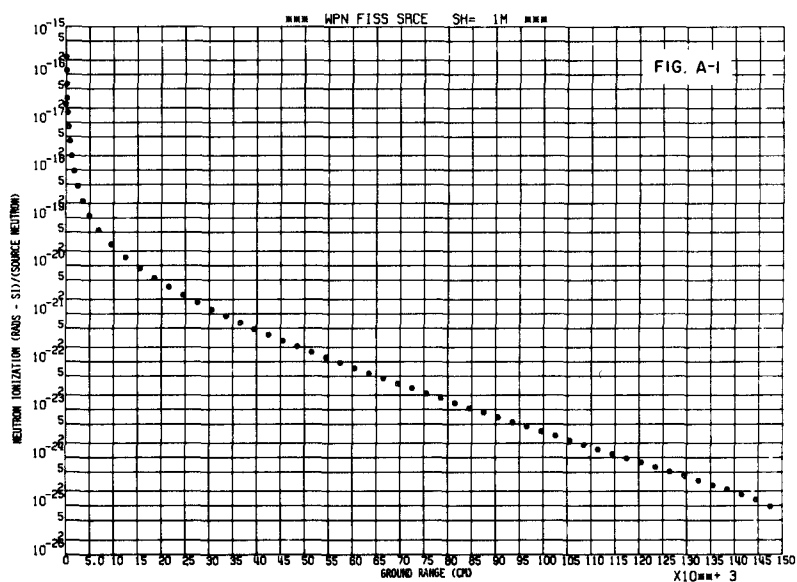
1. E. A. Straker, "Time-Dependent Neutron and Secondary Gamma-Ray Transport in an Air-Over-Ground Geometry, Vol. II, Tabulated Data," ORNL-4289 (September 1968).
2. E. A. Straker, M. B. Emmett, B. J. McGregor, J. V. Pace, III, R. W. Roussin, H. T. Smith, and L. R. Williams, "Investigation of the Adequacy of Nitrogen Cross-Section Sets: Comparison of Neutron and Secondary Gamma-Ray Transport Calculations with Integral Experiments," ORNL-TM-3268 (1972).
3. J. E. Campbell, H. A. Sandmeier, "Radiation Transport in Air-Over-Ground and Air-Over-Seawater for Application to Low-Altitude, Low-Yield Tactical Nuclear Detonations," NWEF Report 1102 (April 1973).
4. E. A. Straker, "The Effect of the Ground on the Steady-State and Time-Dependent Transport of Neutrons and Secondary Gamma Rays in the Atmosphere," Nucl. Sci. Eng. 46, 334 (1971); see also ORNL-TM-3754 (1972).
5. L. Huszar, L. J. Nessler, and W. T. Woolson, "User's Guide to Version 2 of ATR (Air Transport of Radiation)," DNA 3144Z (SAI-73-534-LJ) (April 1973).
6. W. A. Rhoades et al., "The DOT III Two-Dimensional Discrete Ordinates Transport Code," ORNL-TM-4280 (1973).
7. N. M. Greene, J. L. Lucius, W. E. Ford, III, J. E. White, R. Q. Wright, and L. M. Petrie, "AMPX: A Modular Code System for Generating Coupled Multigroup Neutron-Gamma Libraries from ENDF/B," ORNL-TM-3706 (AMPX-1) (to be published).
8. W. W. Engle, "A User's Manual for ANISN - A One-Dimensional Discrete Ordinates Transport Code with Anisotropic Scattering," K-1693, Union Carbide Corporation (1967).
9. E. A. Straker and M. L. Gritzner, "Neutron and Secondary Gamma-Ray Transport in Infinite Homogeneous Air," ORNL-4464 (December 1969).
10. "Protection Against Neutron Radiation," NCRP-38, National Council on Radiation Protection and Measurements, Washington, D. C., 1971.
11. H. C. Claiborne and D. K. Trubey, "Dose Rates in a Slab Phantom from Monoenergetic Gamma Rays," Nucl. Appl. Tech. 8, 450 (1970).

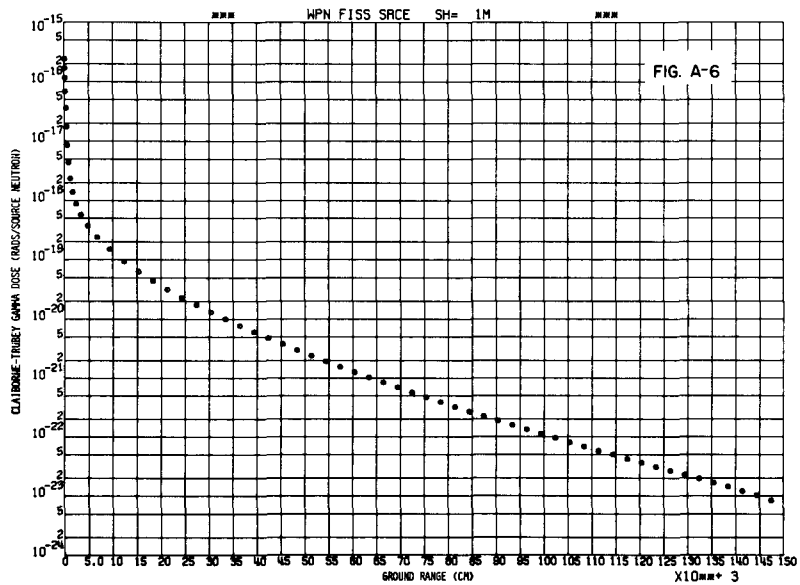
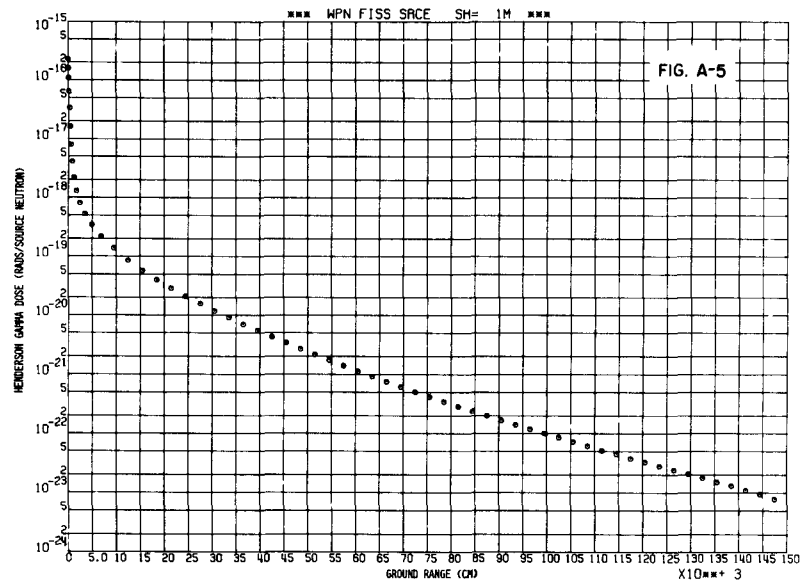
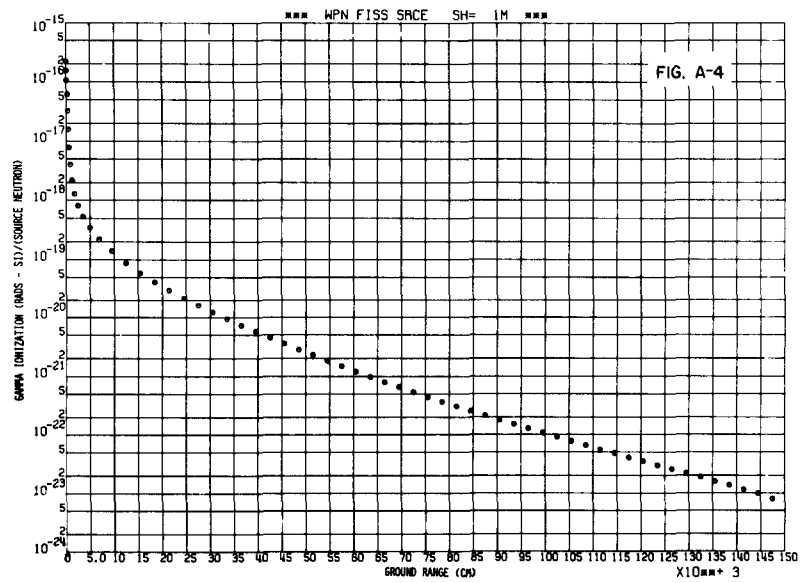
Appendix

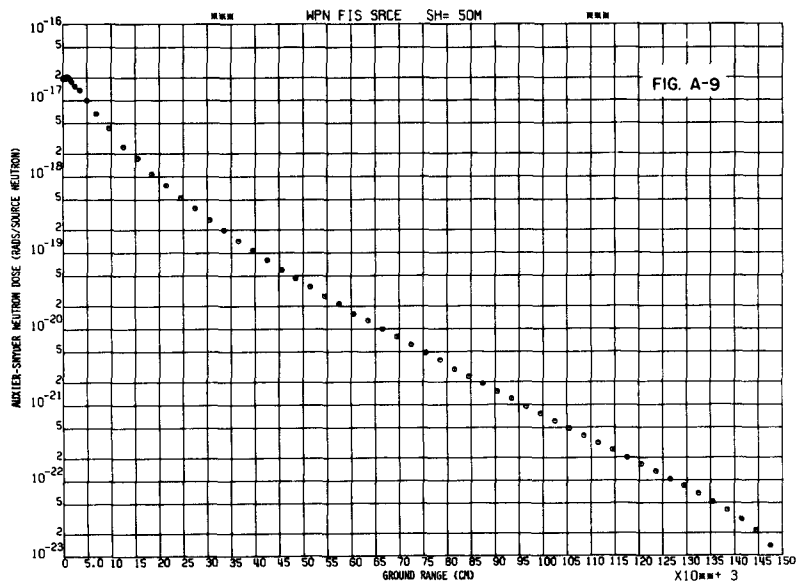
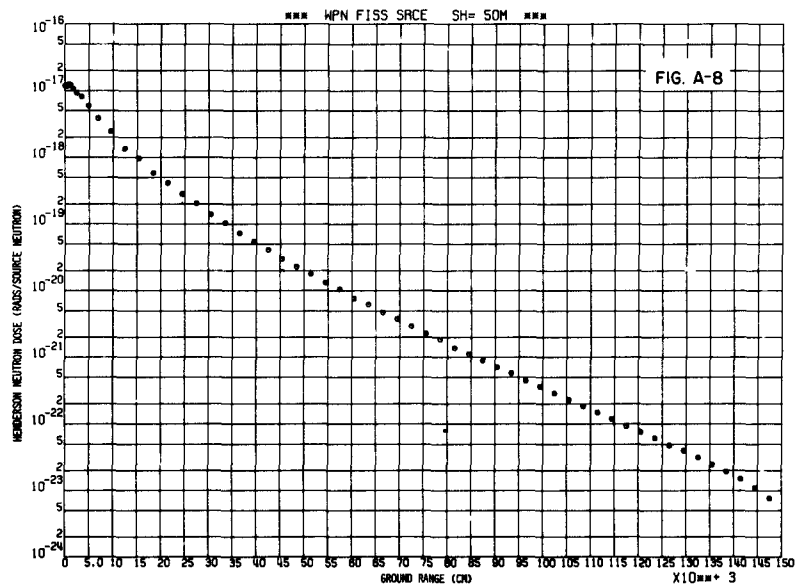
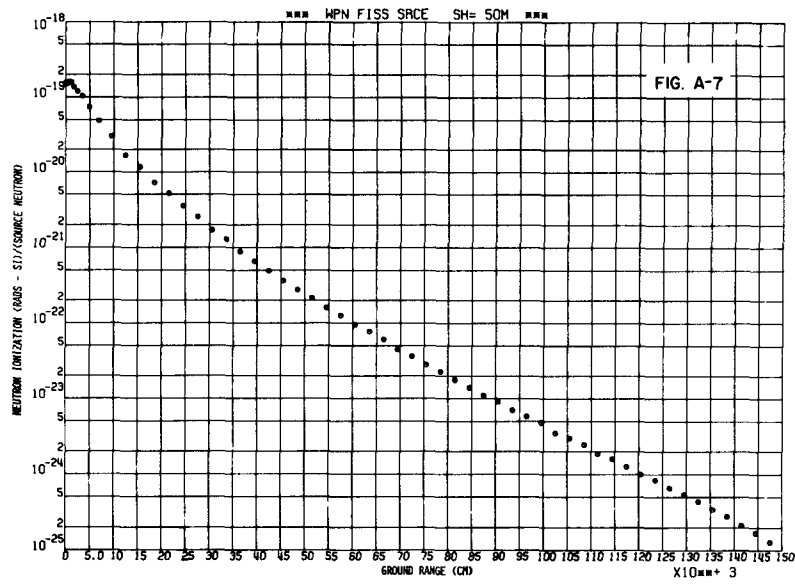
This appendix contains a series of plots of the calculated responses at the air-ground and air-seawater interfaces for the weapon fission neutron source and the 14-MeV neutron source at various heights. The responses included are neutron ionizations, Henderson neutron tissue doses, Auxier-Snyder neutron tissue doses, secondary gamma-ray ionizations, Henderson gamma-ray tissue doses, and Claiborne-Trubey gamma-ray tissue doses. An index to the plots is as follows:

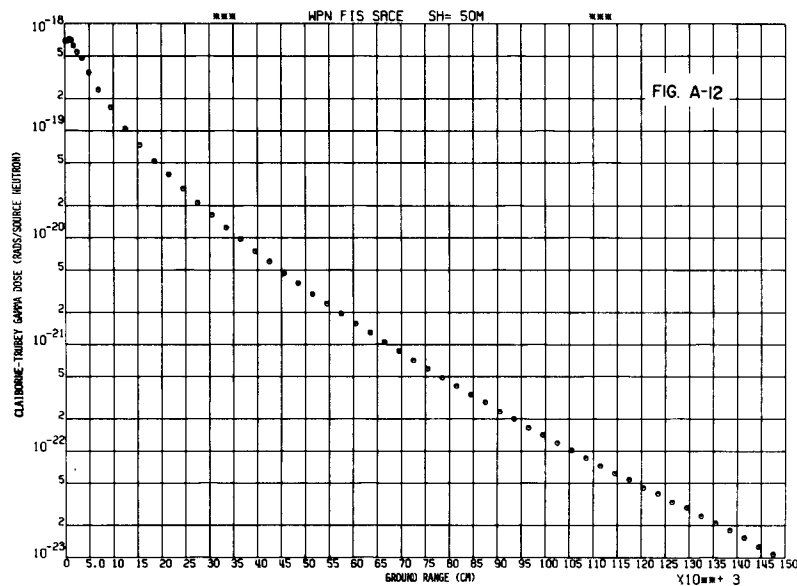
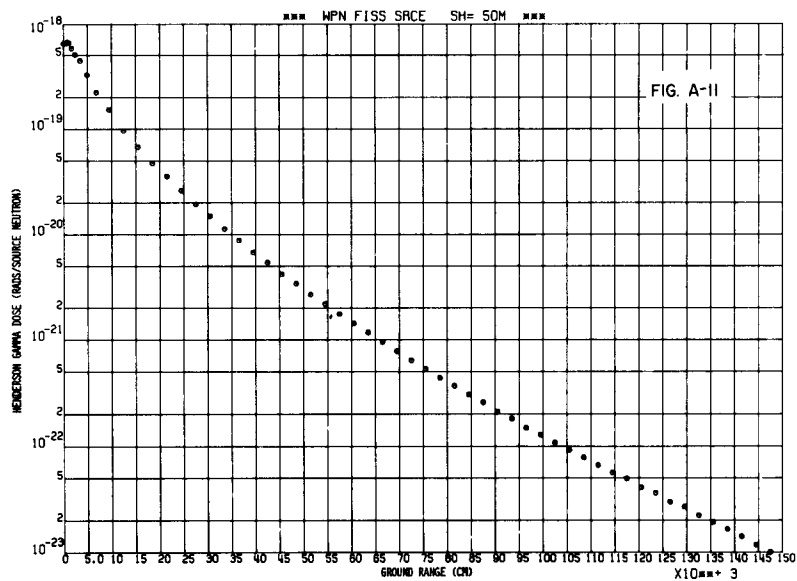
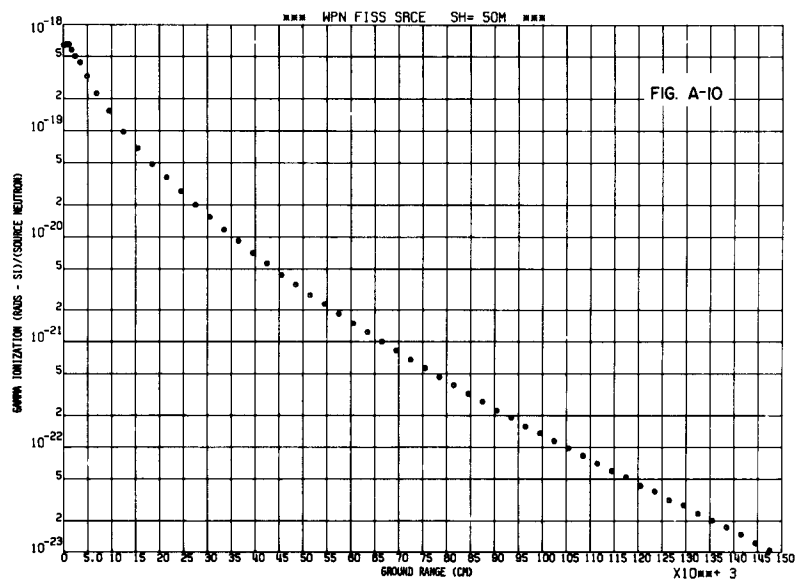
<u>Source</u>	<u>Geometry</u>	<u>Source Height (m)</u>	<u>Response</u>	<u>Fig. No.</u>
Fission	A/G	1	Neutron ionization	A-1
			Henderson neutron tissue dose	A-2
			Auxier-Snyder neutron tissue dose	A-3
			Gamma-ray ionization	A-4
			Henderson gamma-ray tissue dose	A-5
			Claiborne-Trubey gamma-ray tissue dose	A-6
		50	Neutron ionization	A-7
			Henderson neutron tissue dose	A-8
			Auxier-Snyder neutron tissue dose	A-9
			Gamma-ray ionization	A-10
			Henderson gamma-ray tissue dose	A-11
			Claiborne-Trubey gamma-ray tissue dose	A-12
		100	Neutron ionization	A-13
			Henderson neutron tissue dose	A-14
			Auxier-Snyder neutron tissue dose	A-15
			Gamma-ray ionization	A-16
			Henderson gamma-ray tissue dose	A-17
			Claiborne-Trubey gamma-ray tissue dose	A-18
		200	Neutron ionization	A-19
			Henderson neutron tissue dose	A-20
			Auxier-Snyder neutron tissue dose	A-21
			Gamma-ray ionization	A-22
			Henderson gamma-ray tissue dose	A-23
			Claiborne-Trubey gamma-ray tissue dose	A-24
		300	Neutron ionization	A-25
			Henderson neutron tissue dose	A-26
			Auxier-Snyder neutron tissue dose	A-27
			Gamma-ray ionization	A-28
			Henderson gamma-ray tissue dose	A-29
			Claiborne-Trubey gamma-ray tissue dose	A-30

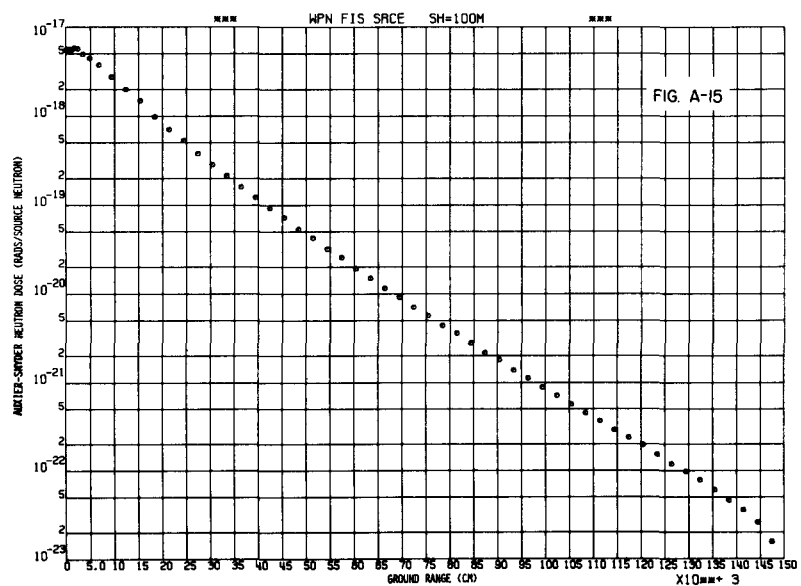
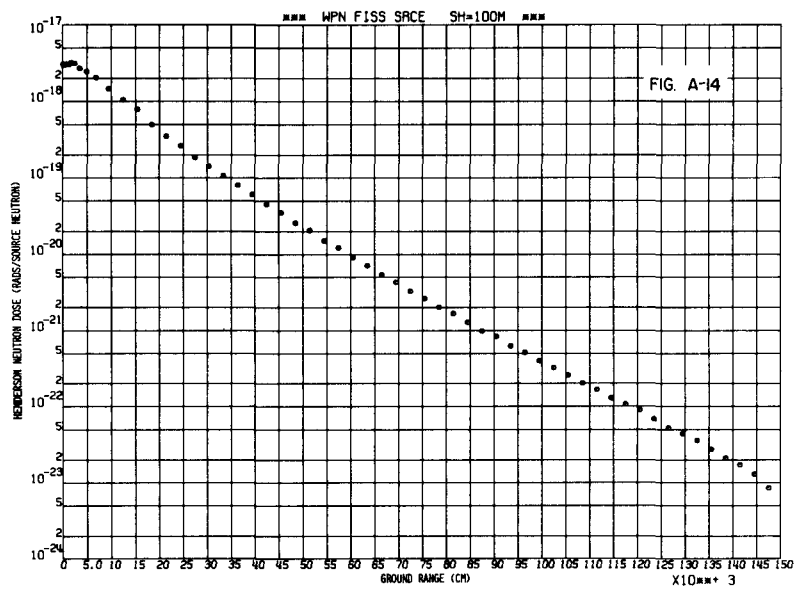
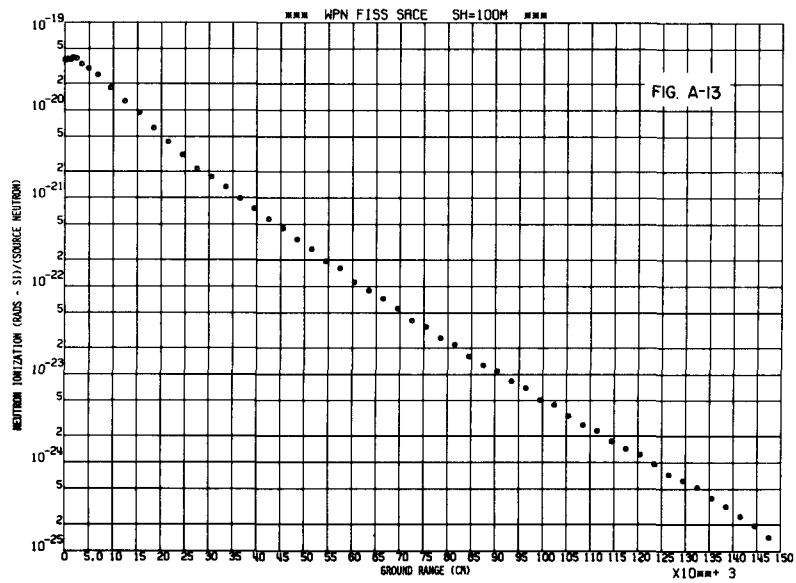
<u>Source</u>	<u>Geometry</u>	<u>Source Height (m)</u>	<u>Response</u>	<u>Fig. No.</u>
14-MeV	A/G	1	Neutron ionization	A-31
			Henderson neutron tissue dose	A-32
			Auxier-Snyder neutron tissue dose	A-33
			Gamma-ray ionization	A-34
			Henderson gamma-ray tissue dose	A-35
			Claiborne-Trubey gamma-ray tissue dose	A-36
		50	Neutron ionization	A-37
			Henderson neutron tissue dose	A-38
			Auxier-Snyder neutron tissue dose	A-39
			Gamma-ray ionization	A-40
			Henderson gamma-ray tissue dose	A-41
			Claiborne-Trubey gamma-ray tissue dose	A-42
		100	Neutron ionization	A-43
			Henderson neutron tissue dose	A-44
			Auxier-Snyder neutron tissue dose	A-45
			Gamma-ray ionization	A-46
			Henderson gamma-ray tissue dose	A-47
			Claiborne-Trubey gamma-ray tissue dose	A-48
		200	Neutron ionization	A-49
			Henderson neutron tissue dose	A-50
			Auxier-Snyder neutron tissue dose	A-51
			Gamma-ray ionization	A-52
			Henderson gamma-ray tissue dose	A-53
			Claiborne-Trubey gamma-ray tissue dose	A-54
		300	Neutron ionization	A-55
			Henderson neutron tissue dose	A-56
			Auxier-Snyder neutron tissue dose	A-57
			Gamma-ray ionization	A-58
			Henderson gamma-ray tissue dose	A-59
			Claiborne-Trubey gamma-ray tissue dose	A-60
Fission	A/SW	50	Neutron Ionization	A-61
			Henderson neutron tissue dose	A-62
			Auxier-Snyder neutron tissue dose	A-63
			Gamma-ray ionization	A-64
			Henderson gamma-ray tissue dose	A-65
			Claiborne-Trubey gamma-ray tissue dose	A-66
14-MeV	A/SW	50	Neutron ionization	A-67
			Henderson neutron tissue dose	A-68
			Auxier-Snyder neutron tissue dose	A-69
			Gamma-ray ionization	A-70
			Henderson gamma-ray tissue dose	A-71
			Claiborne-Trubey gamma-ray tissue dose	A-72

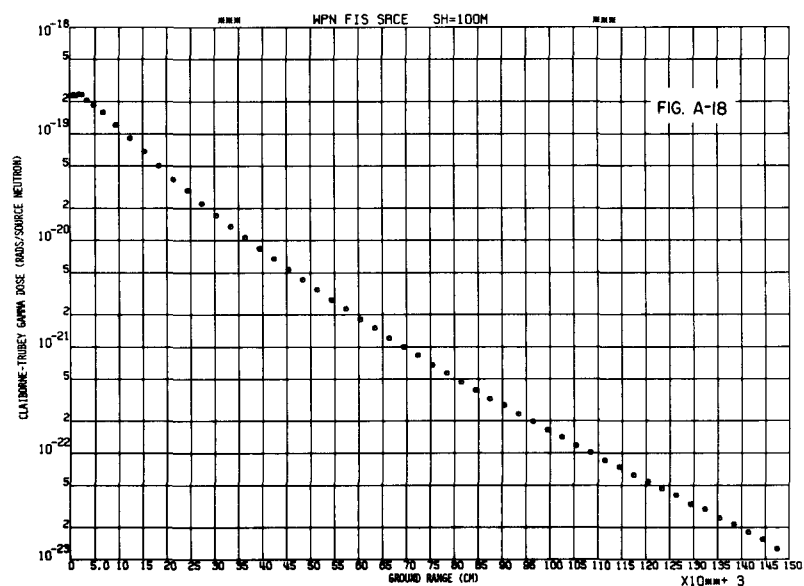
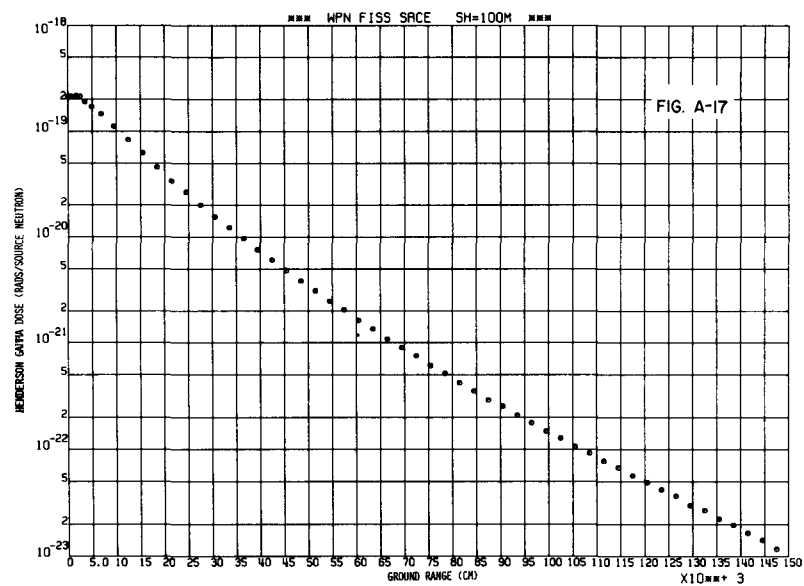
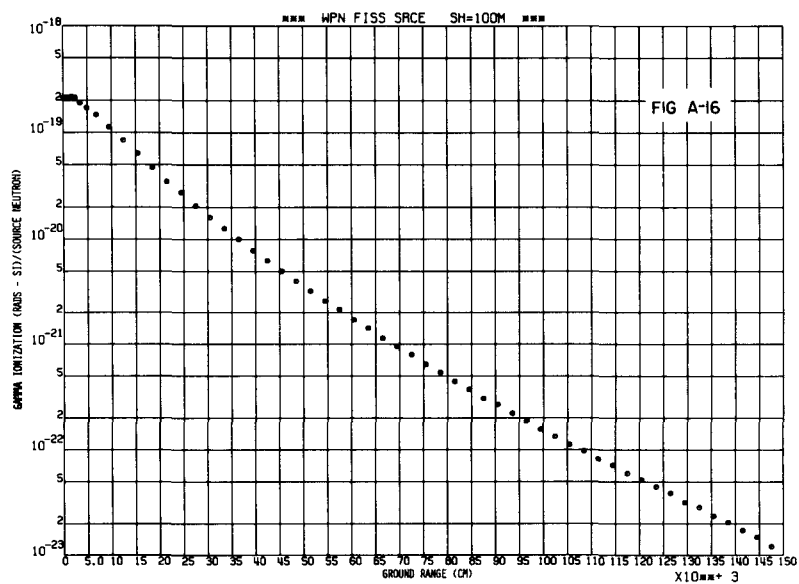


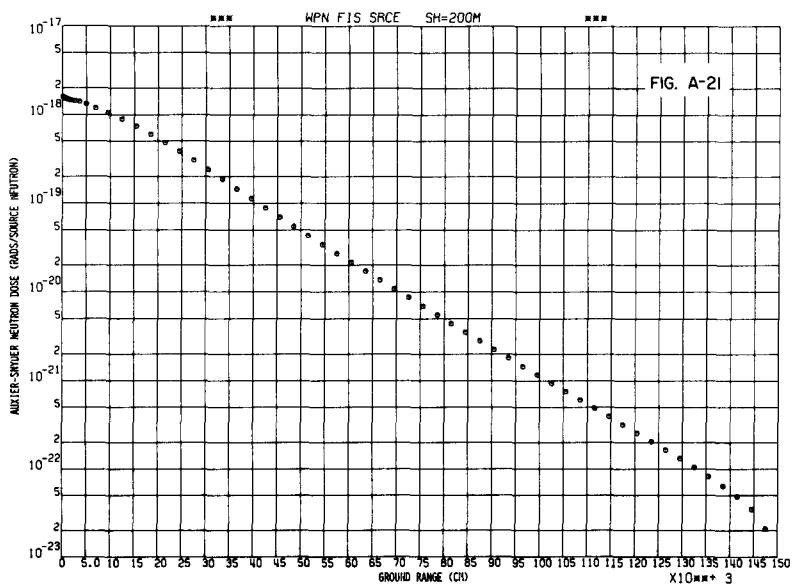
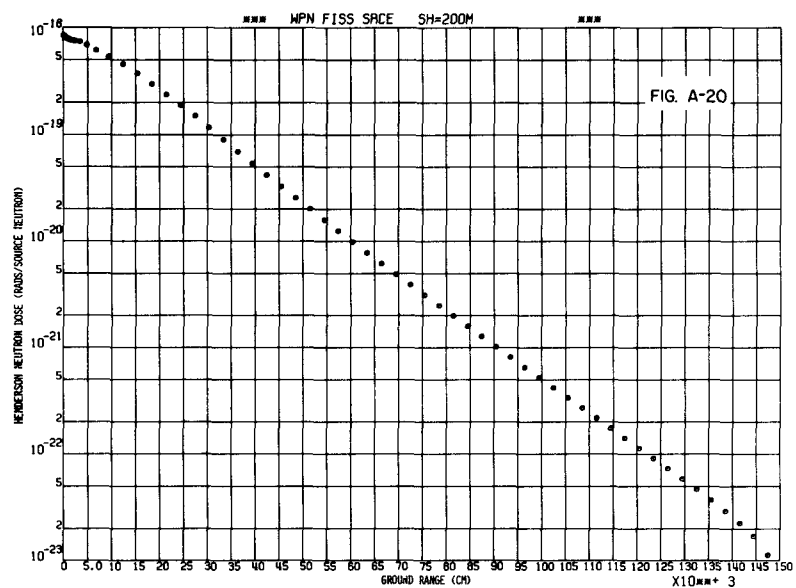
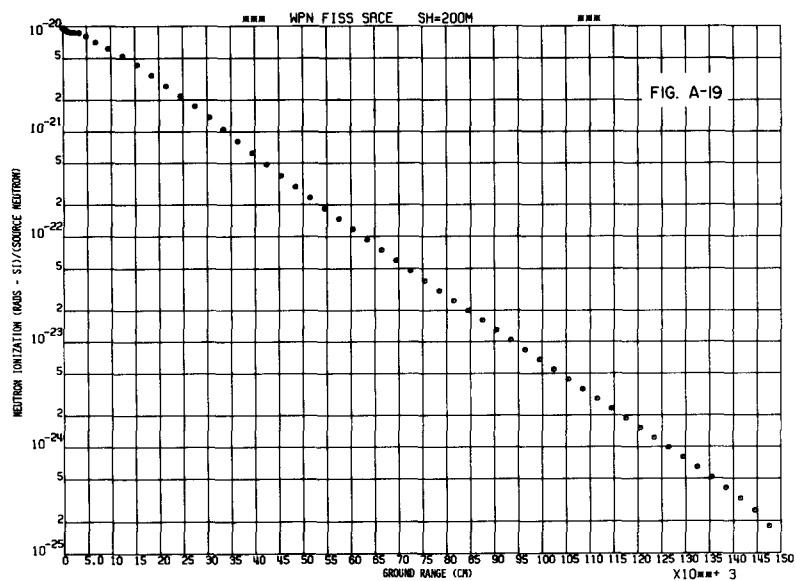


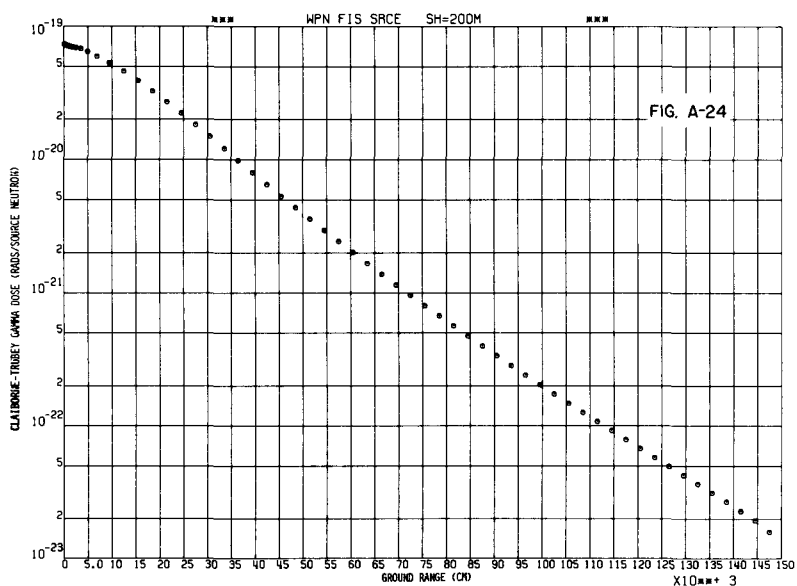
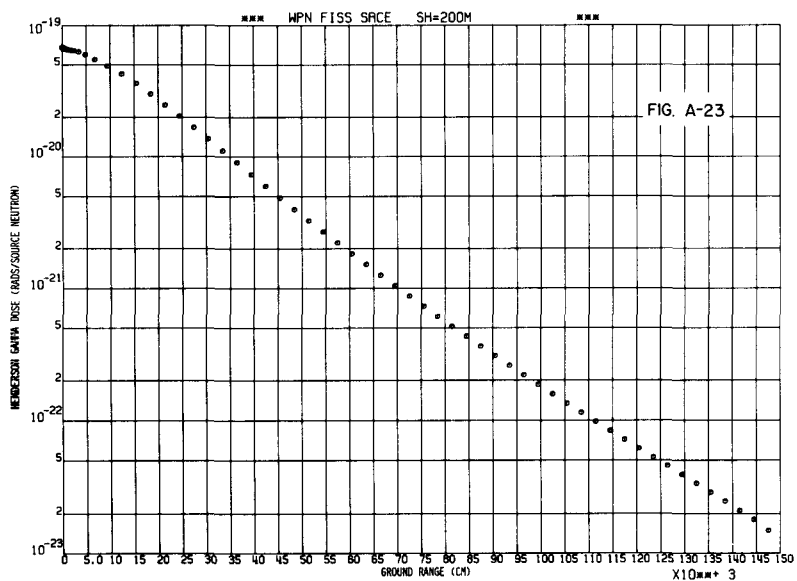
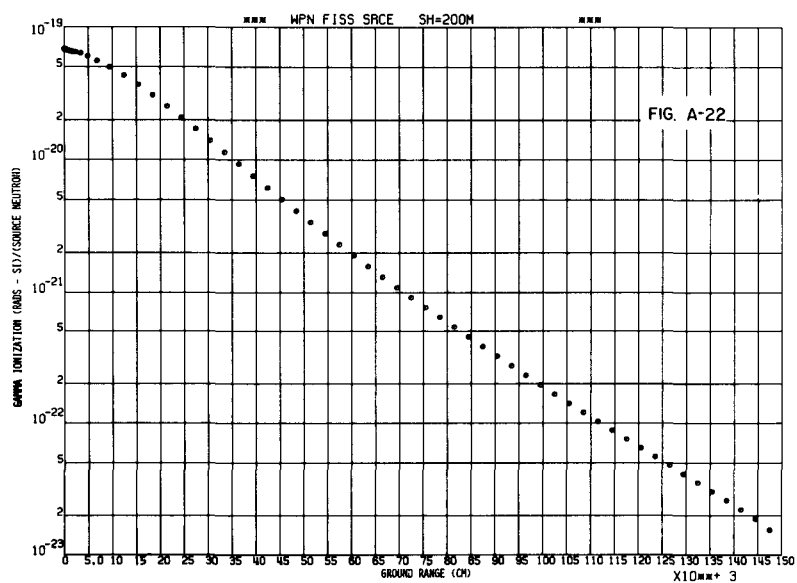


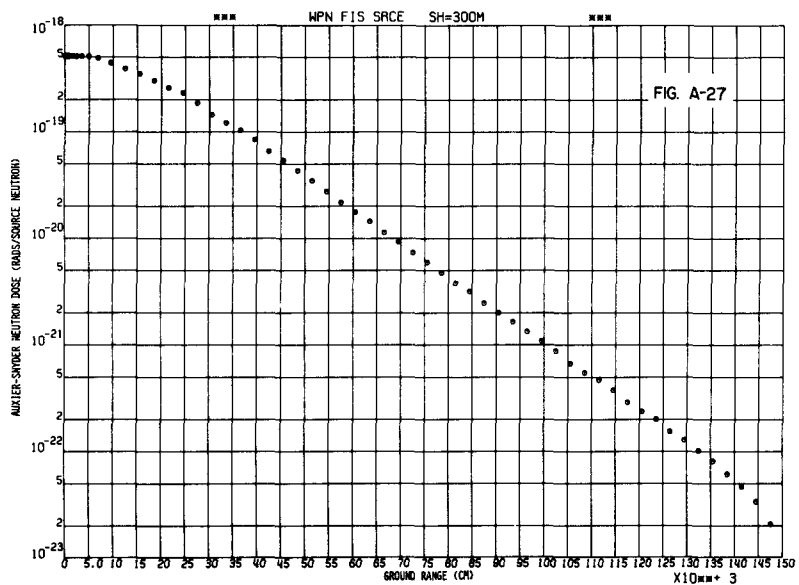
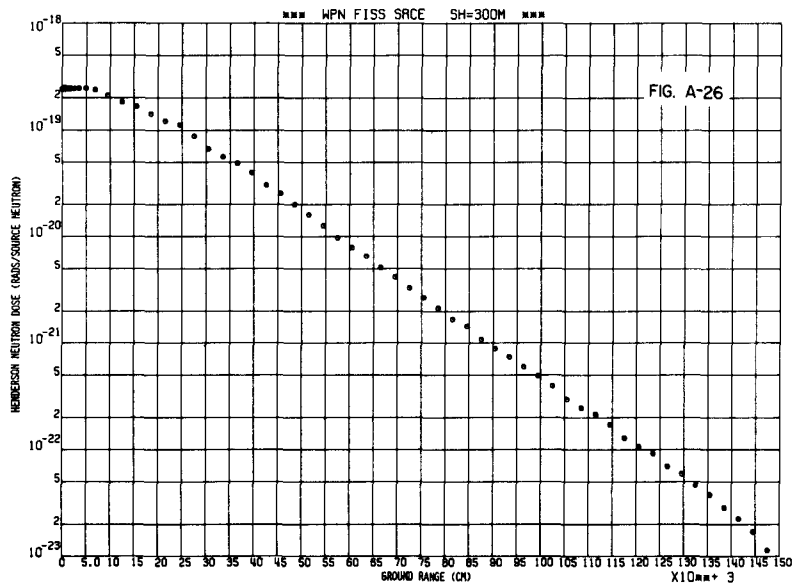
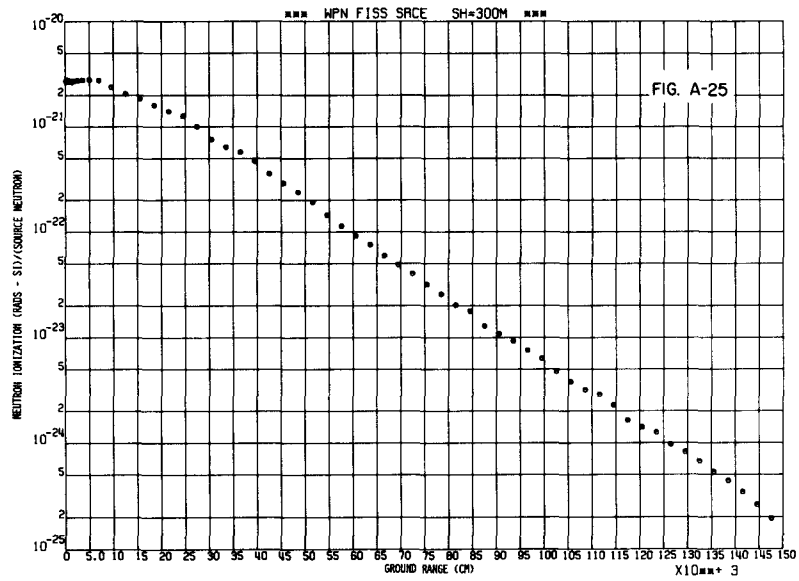


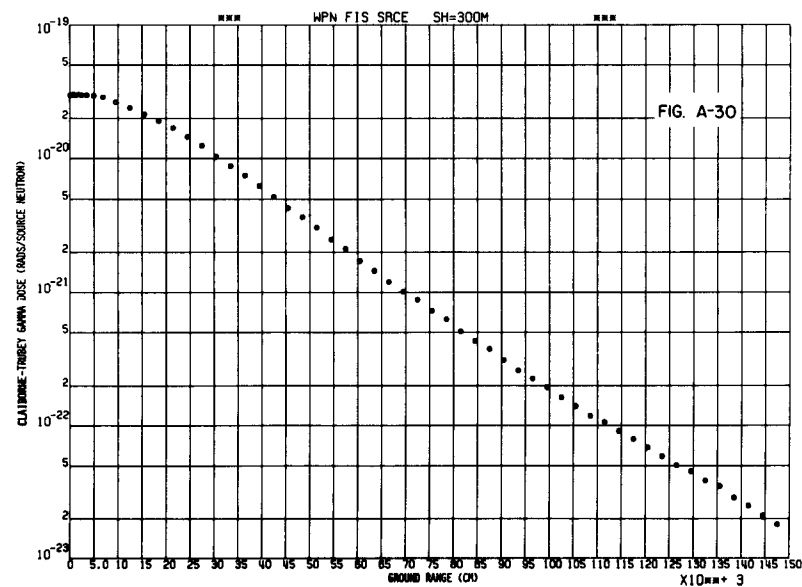
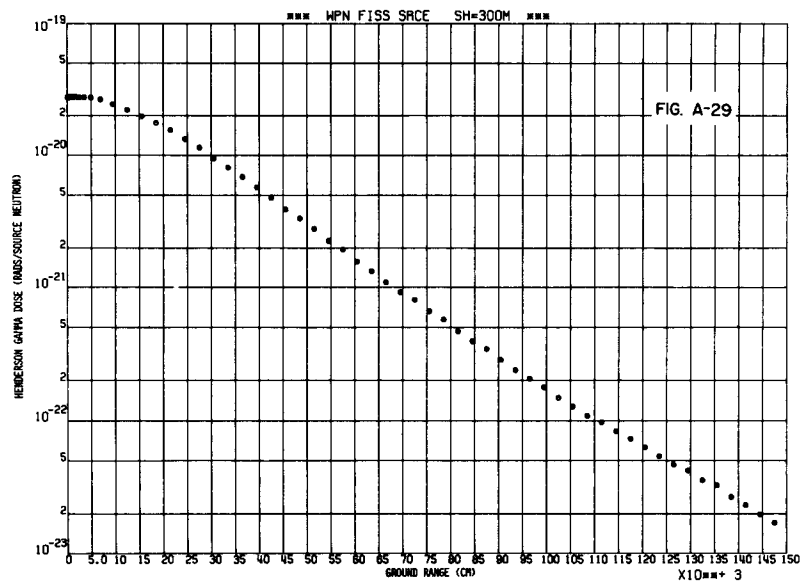
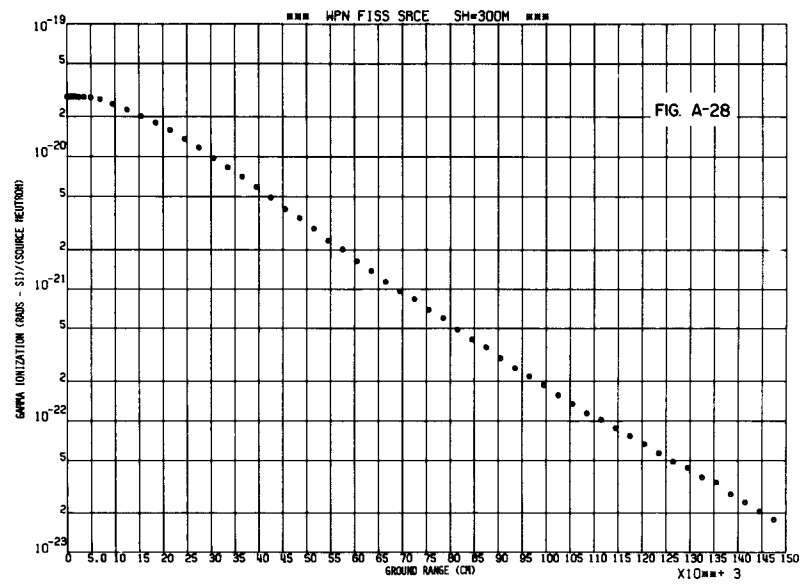


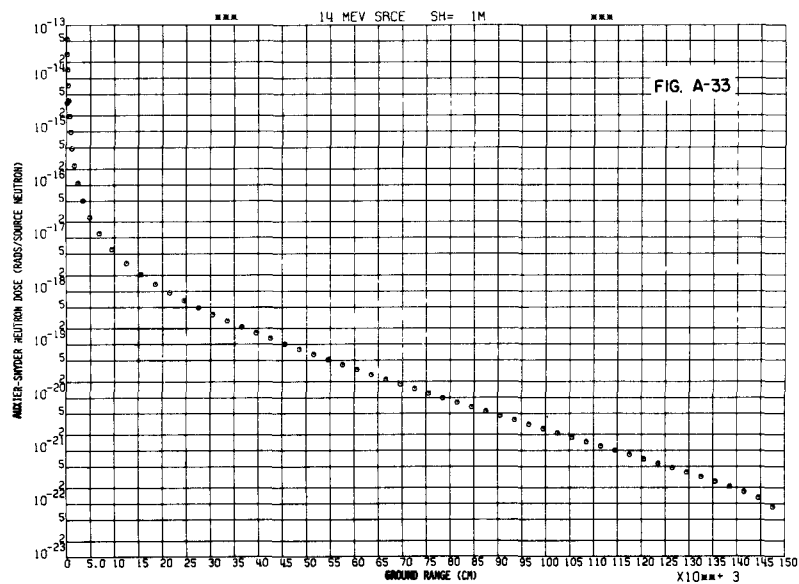
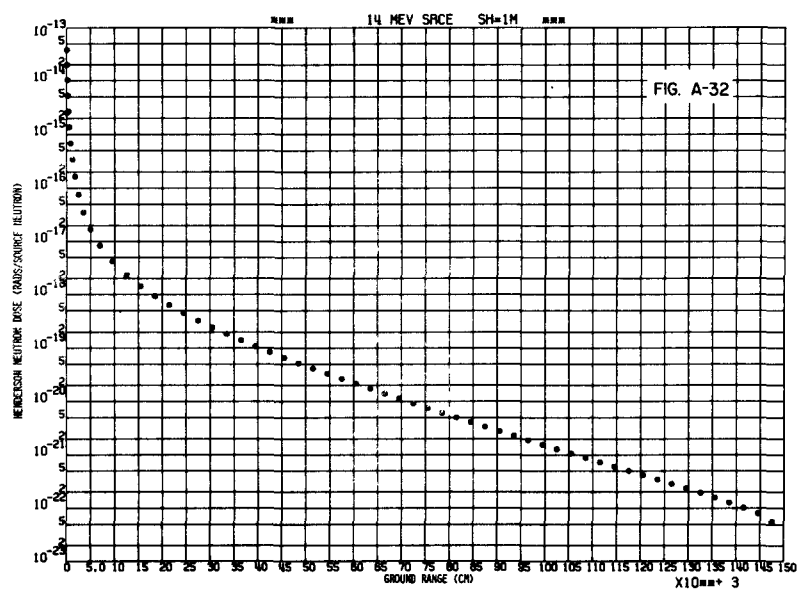
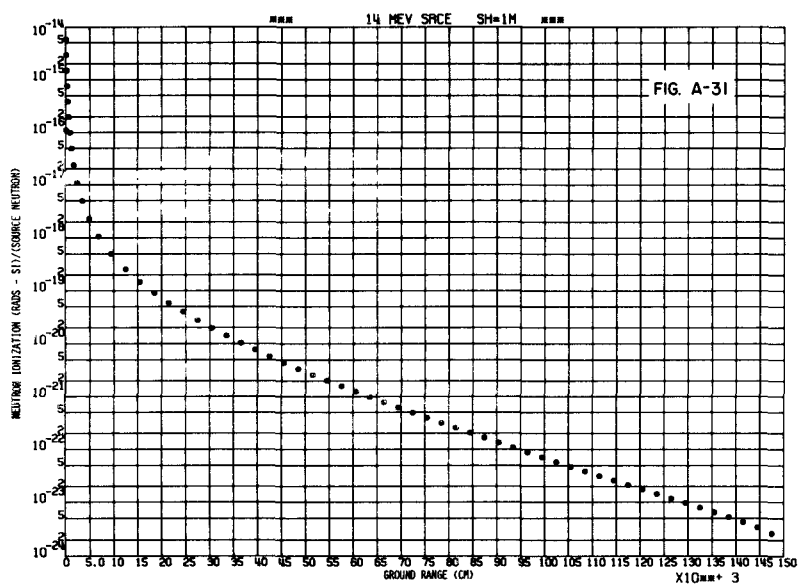


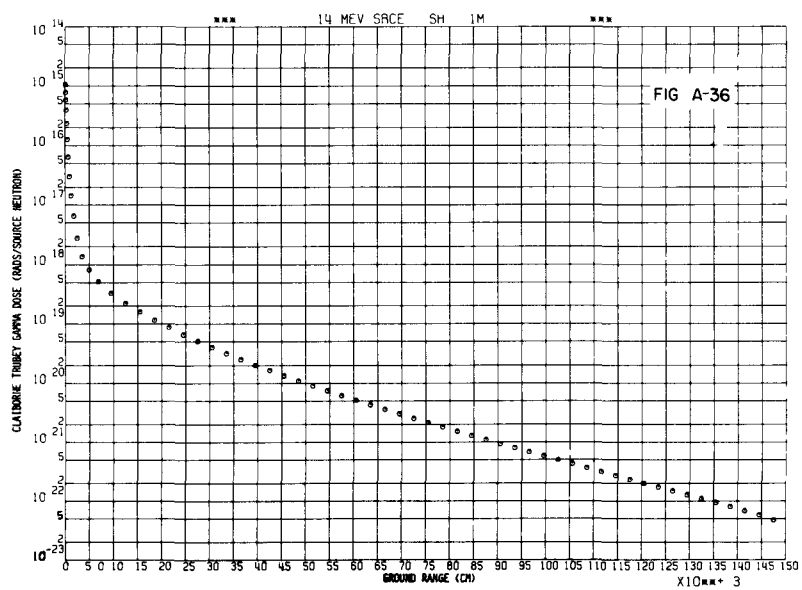
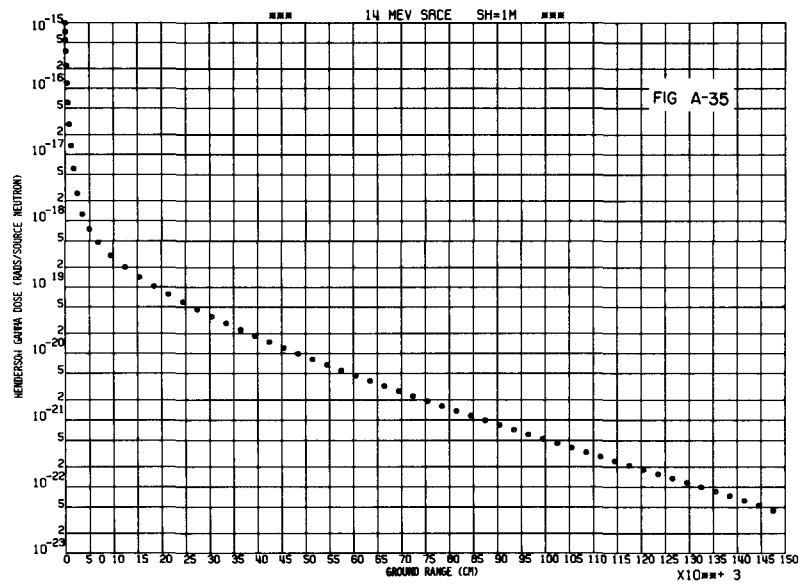
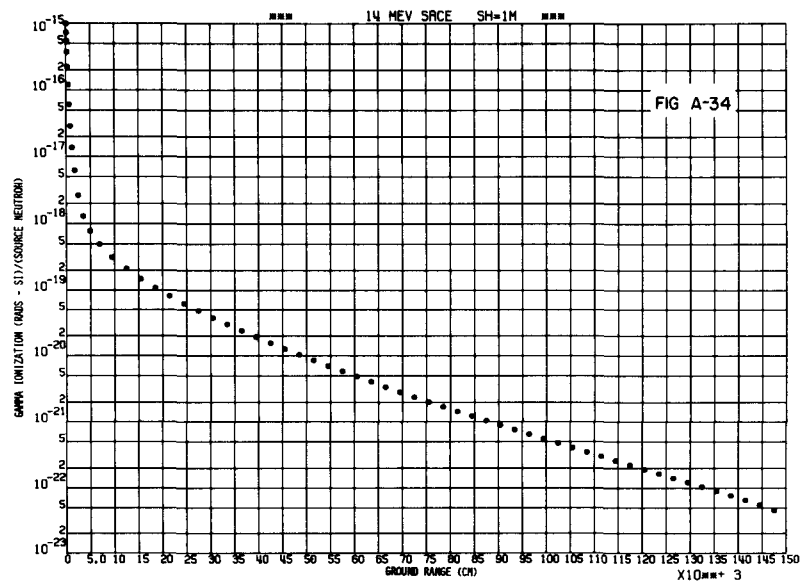


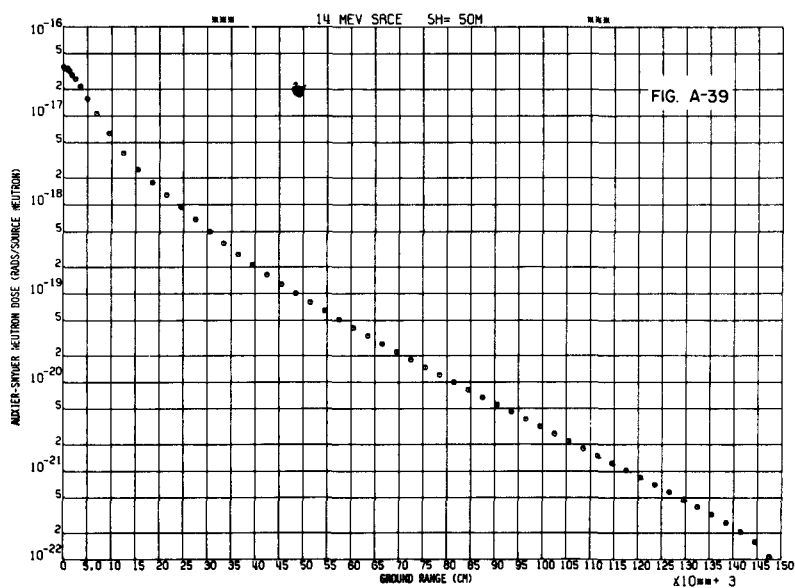
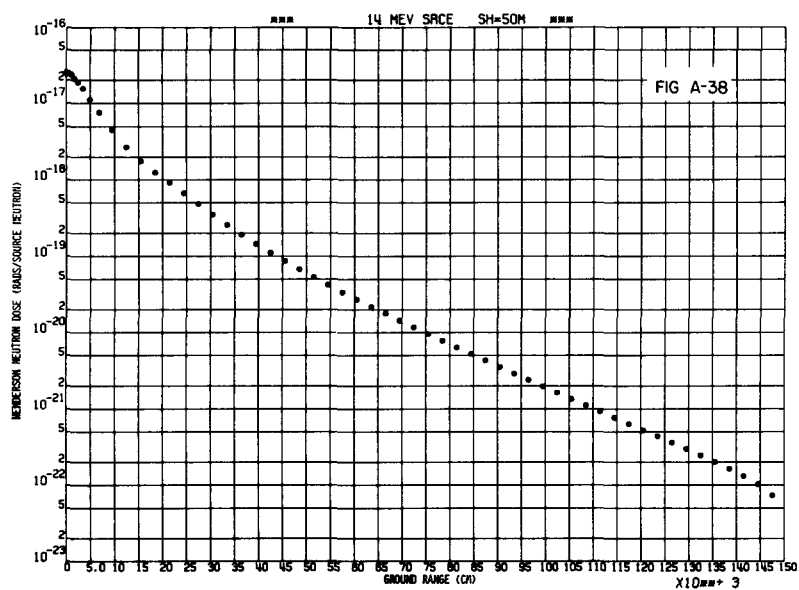
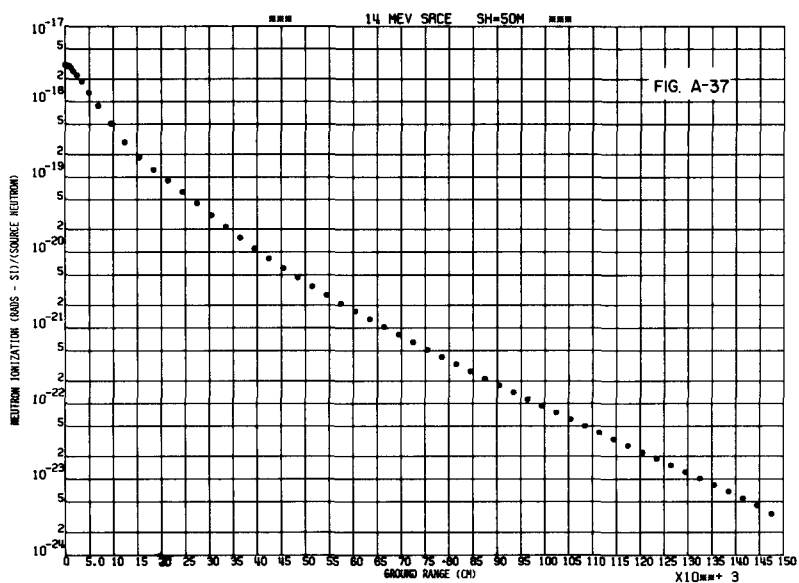


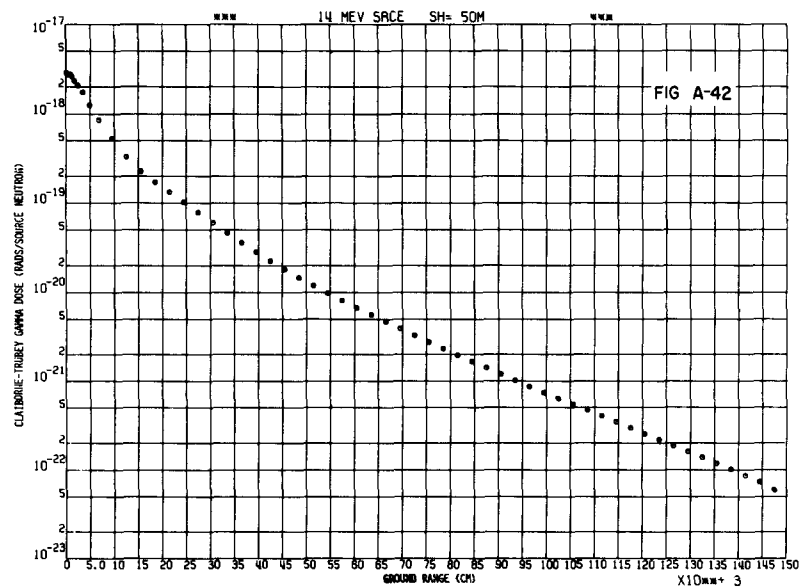
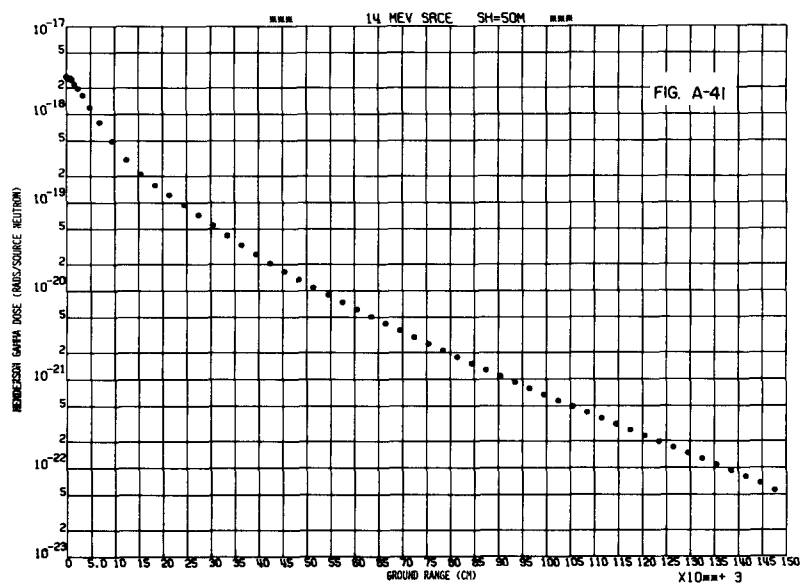
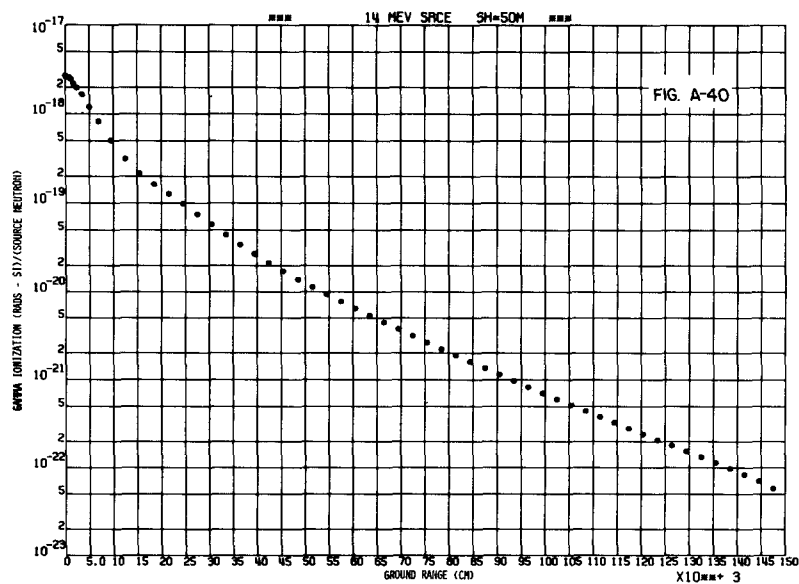


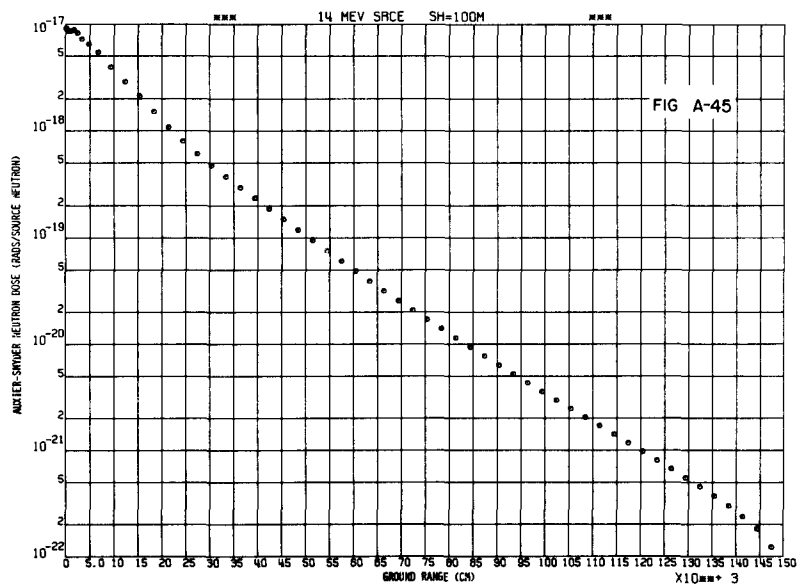
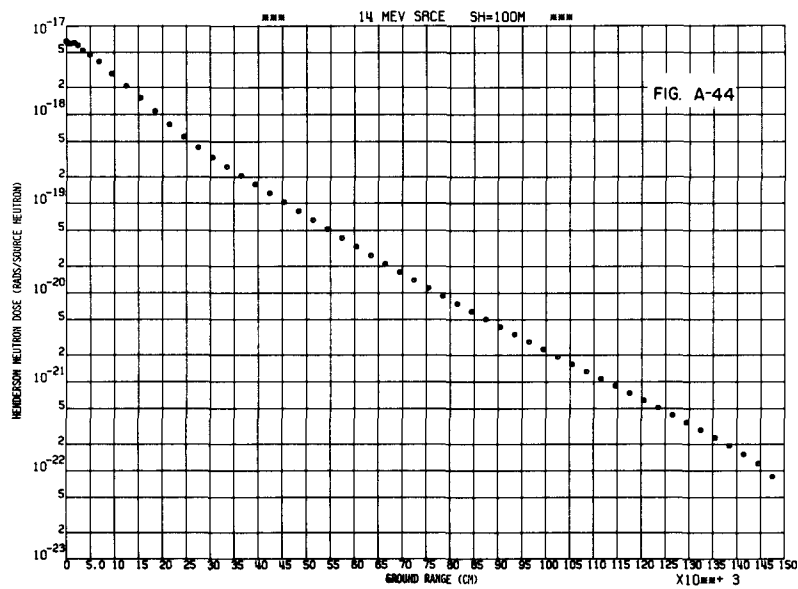
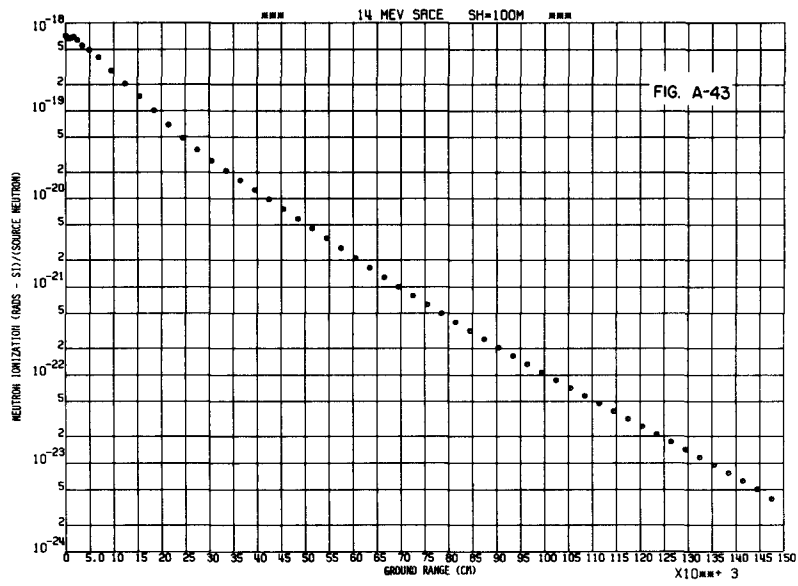


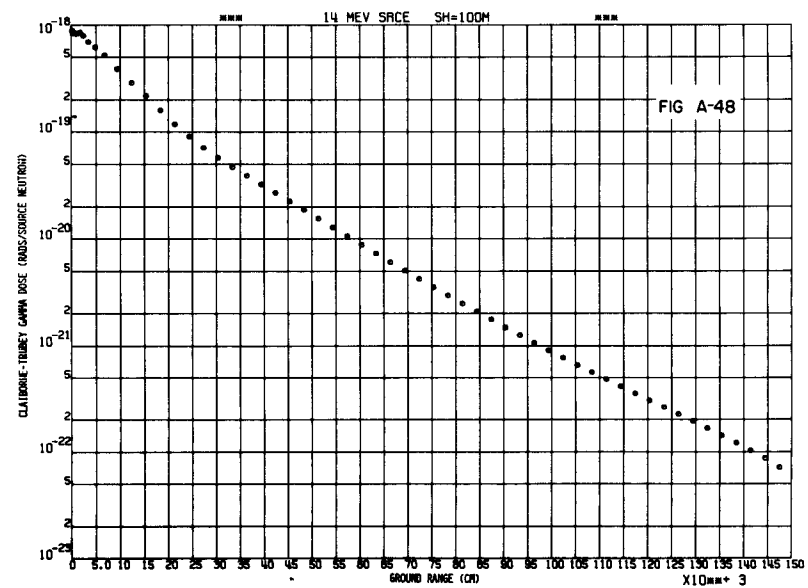
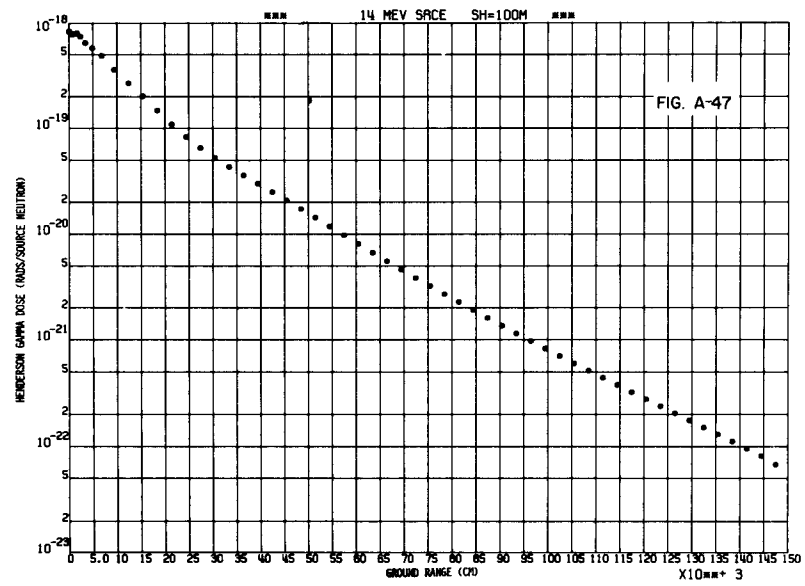
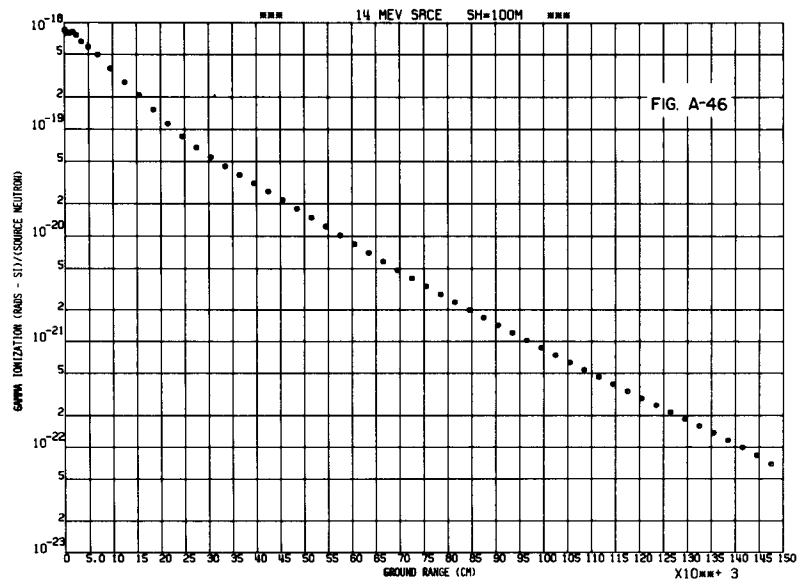


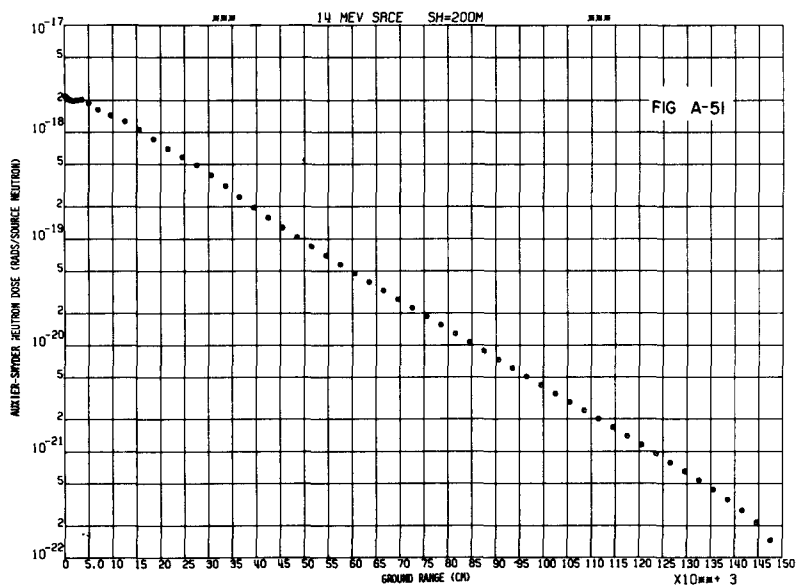
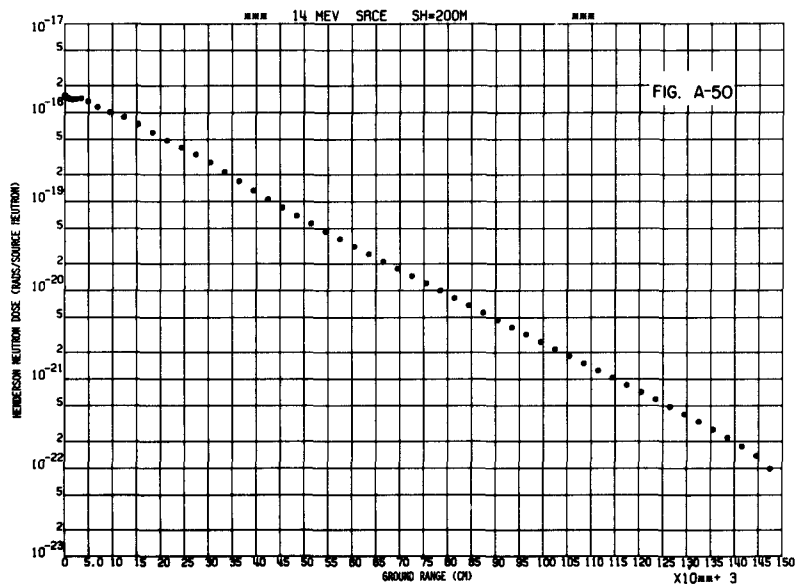
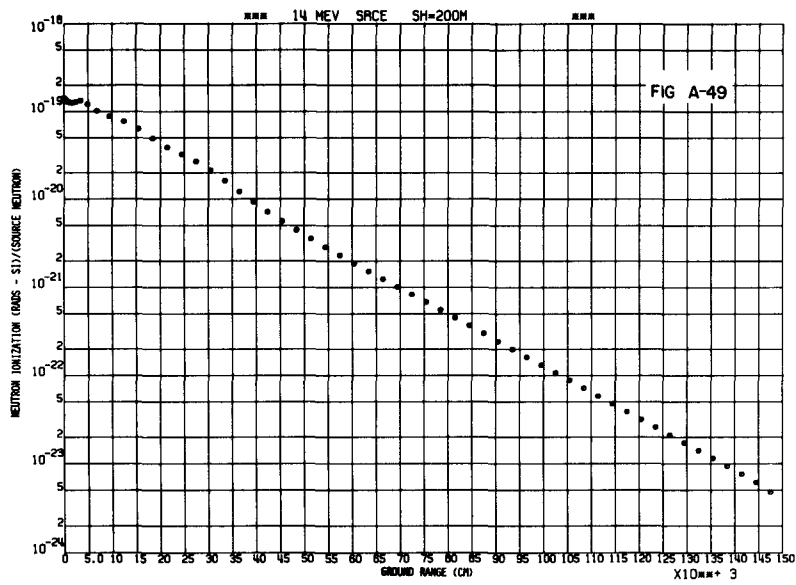


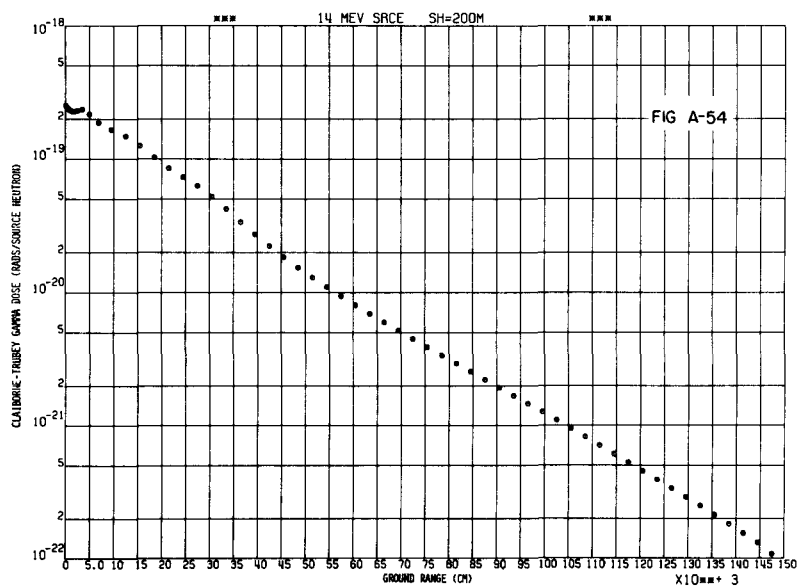
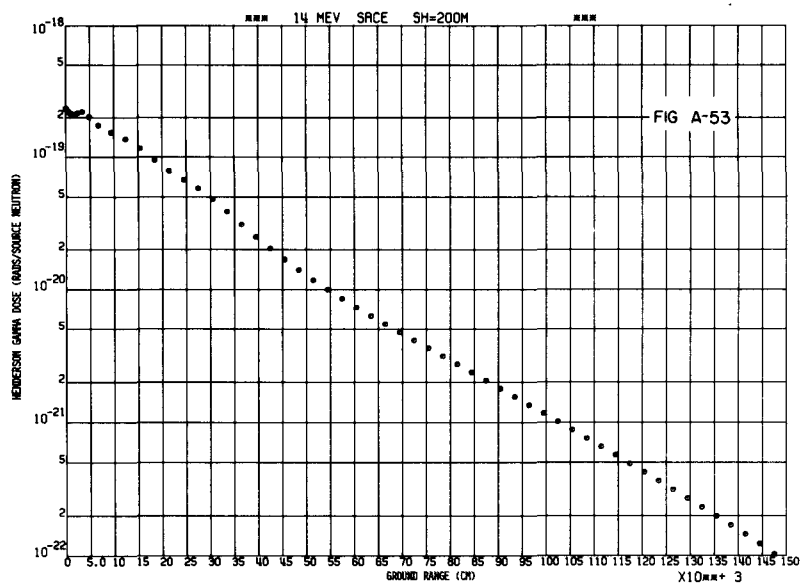
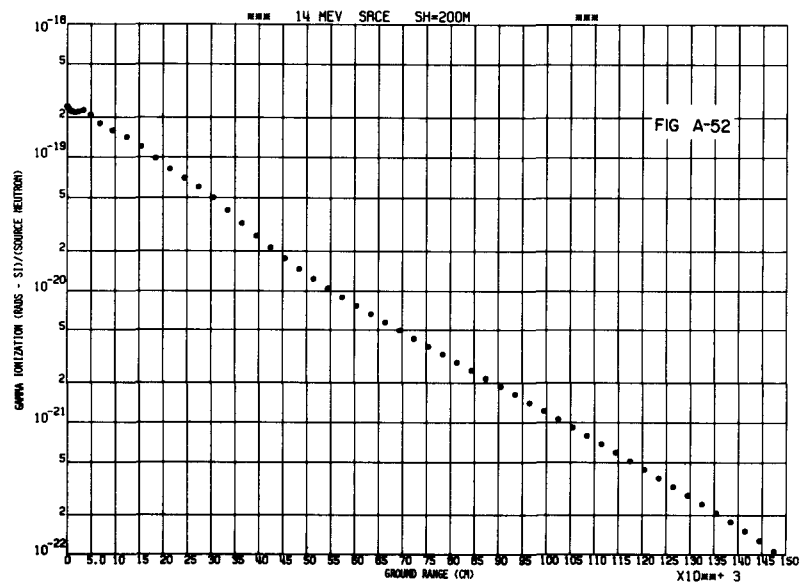


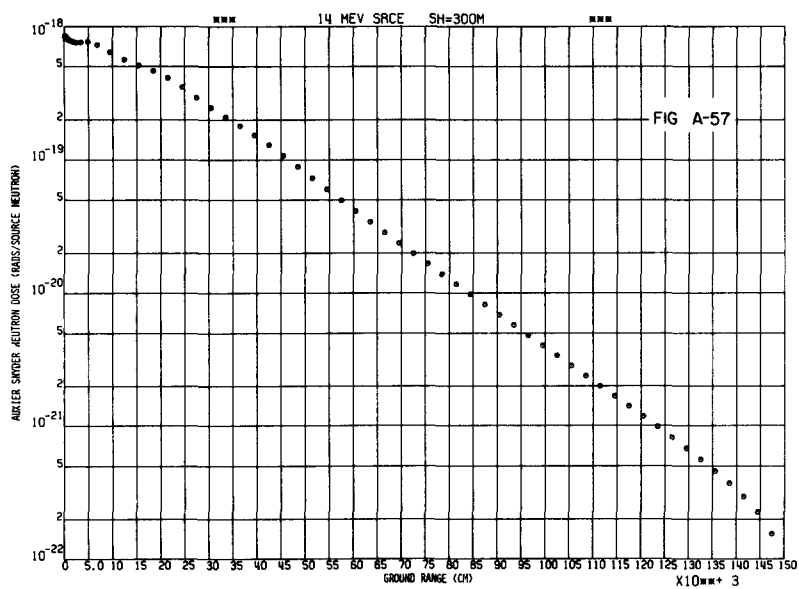
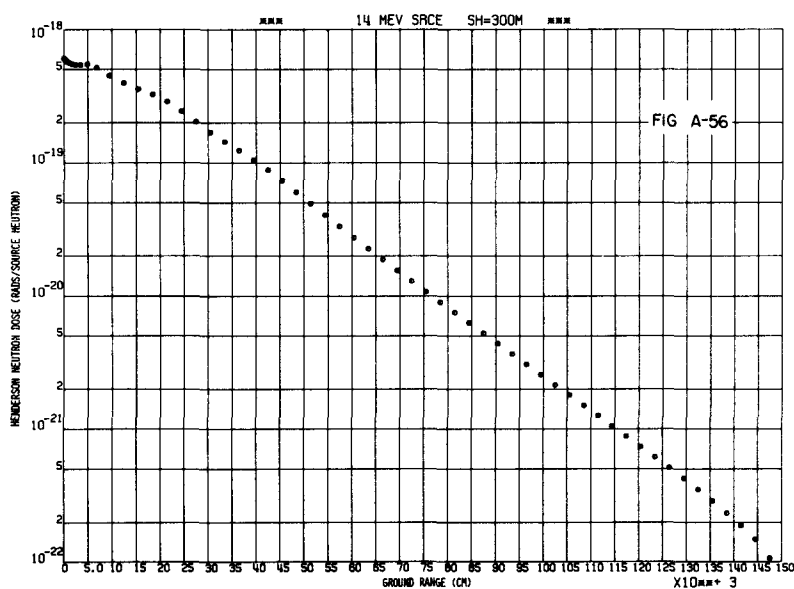
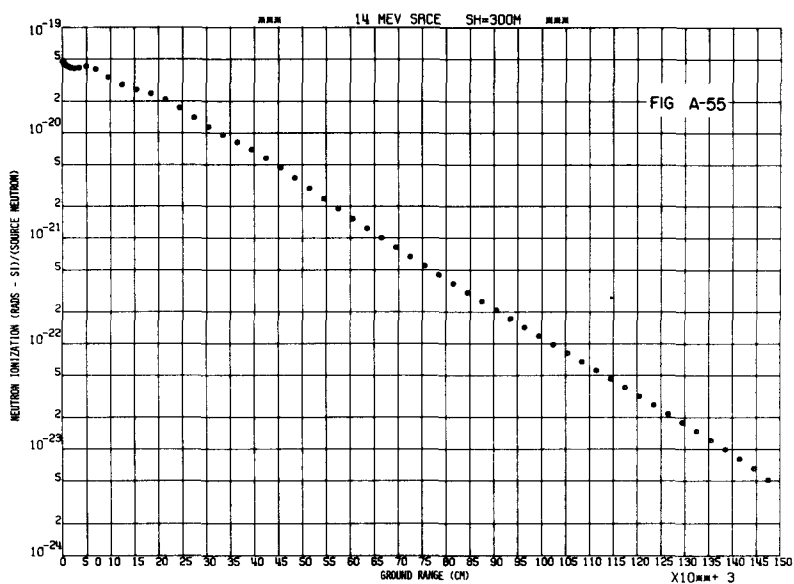


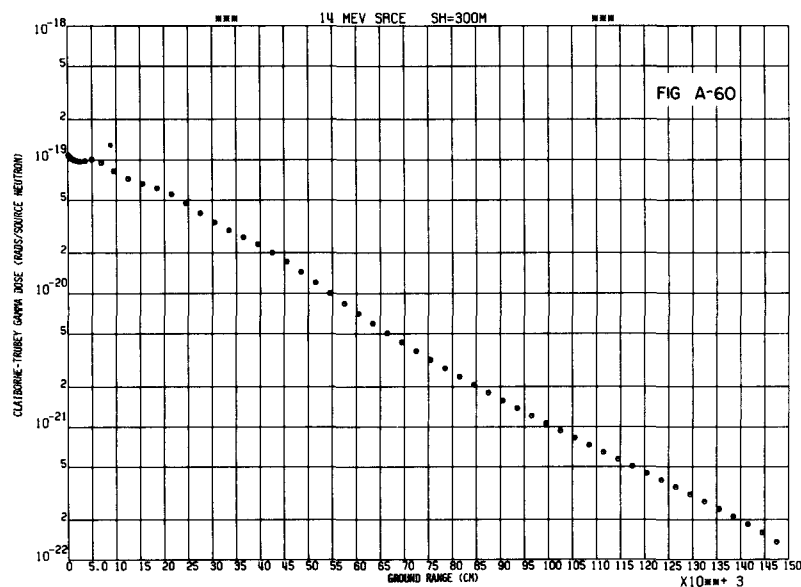
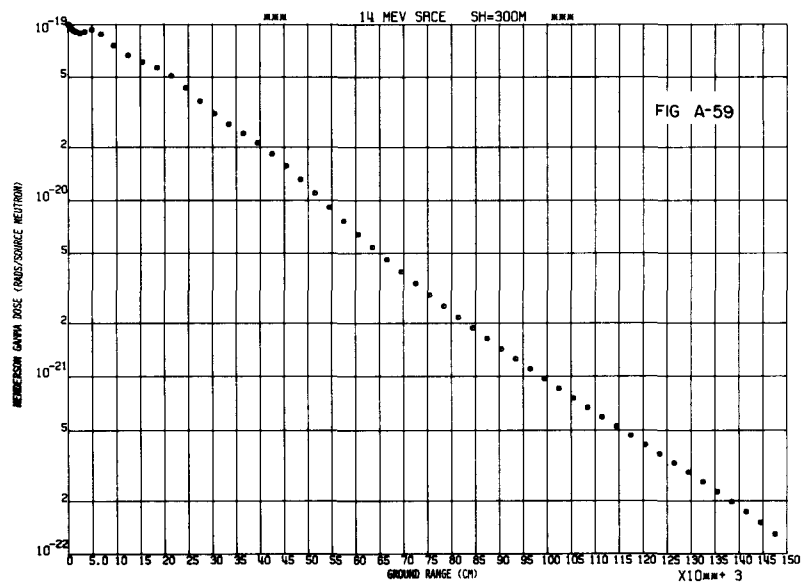
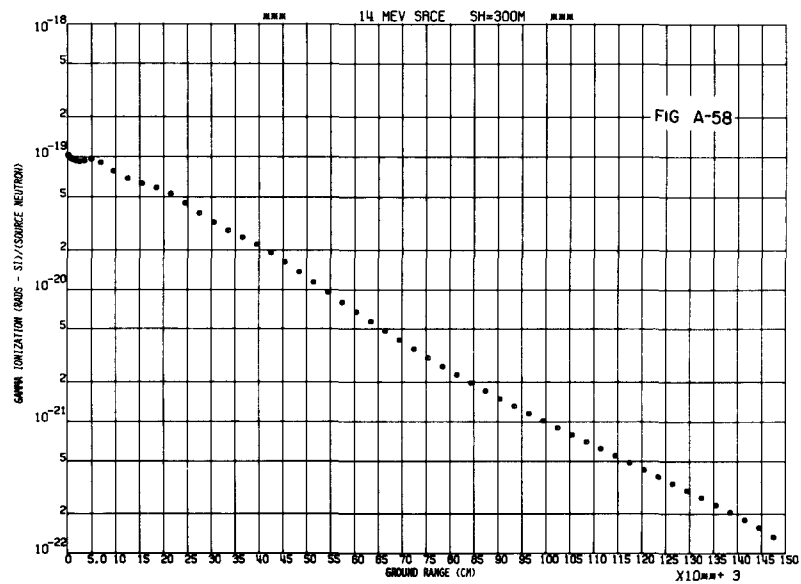


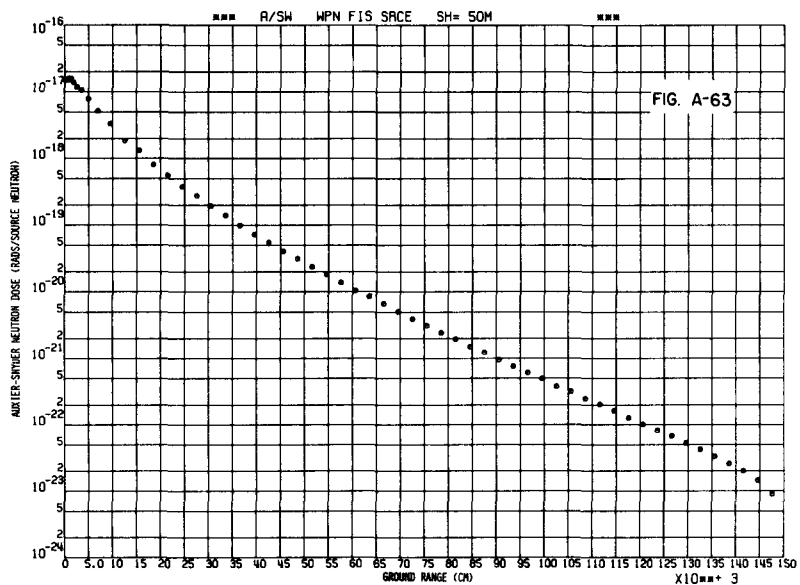
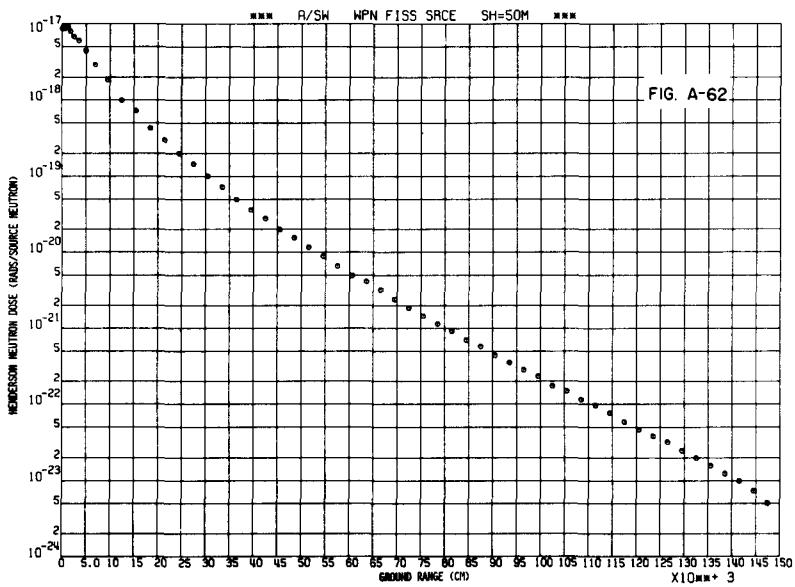
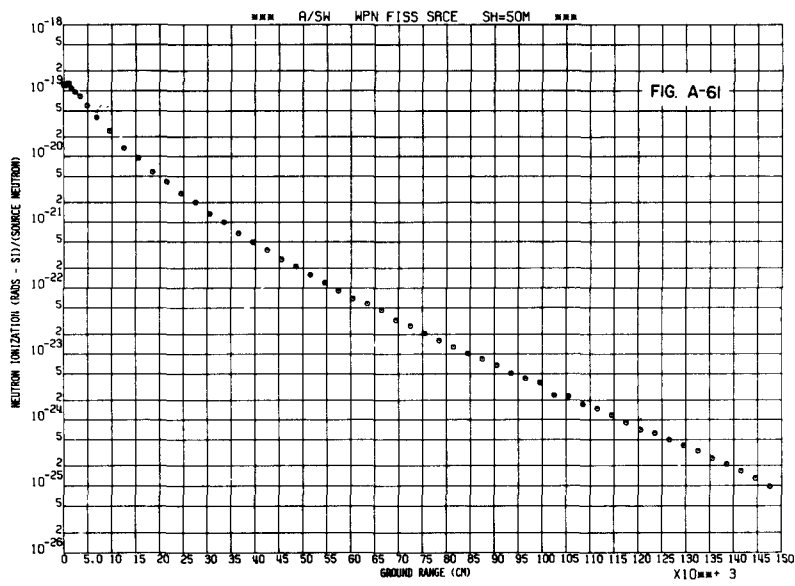


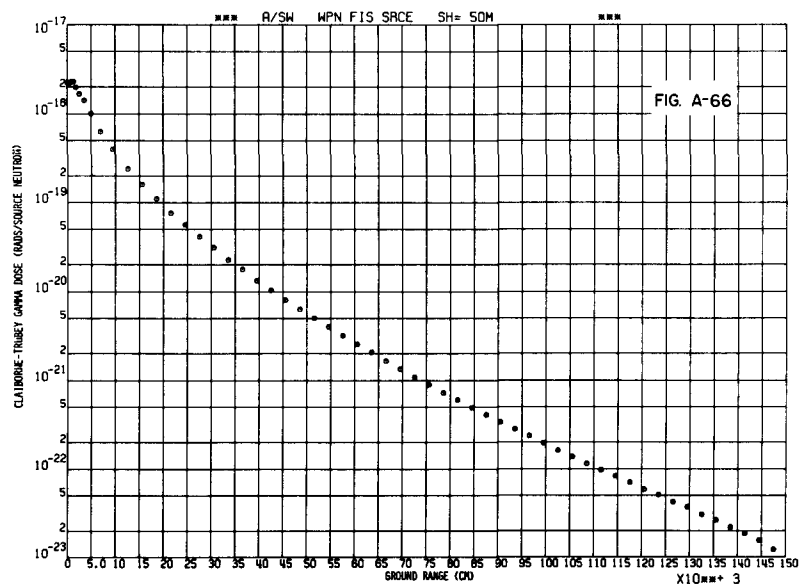
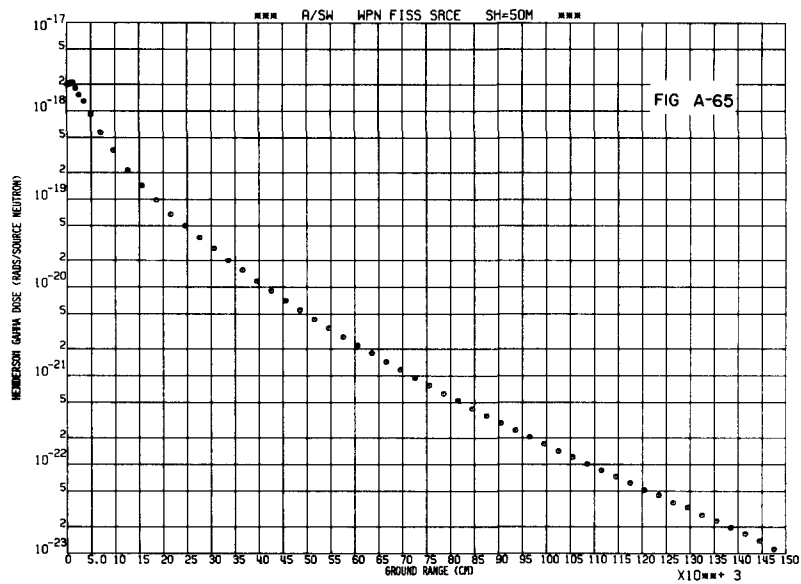
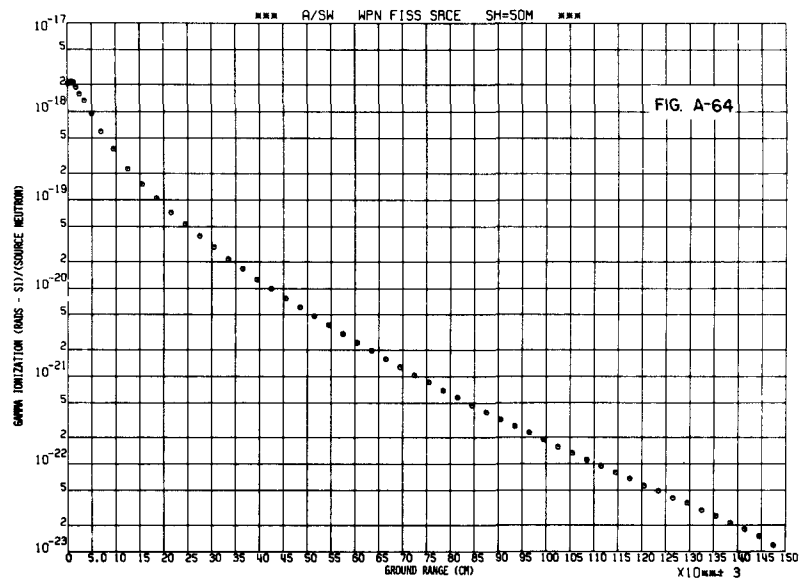


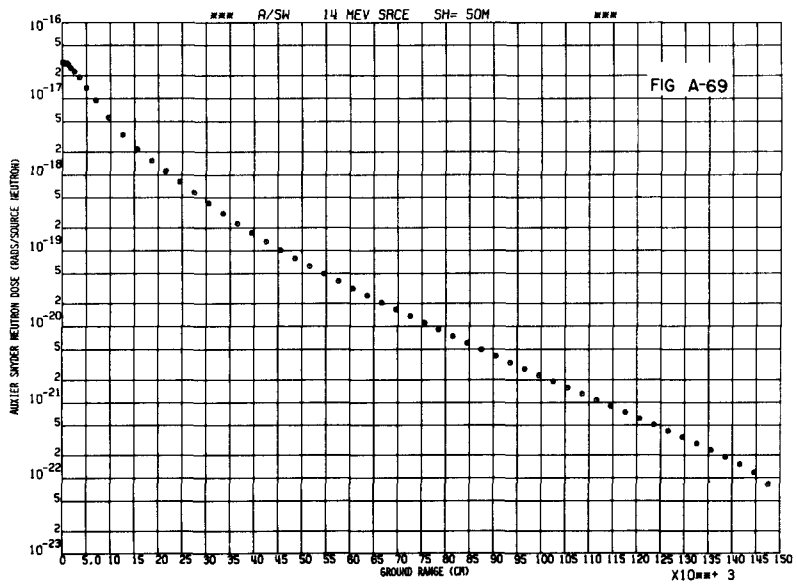
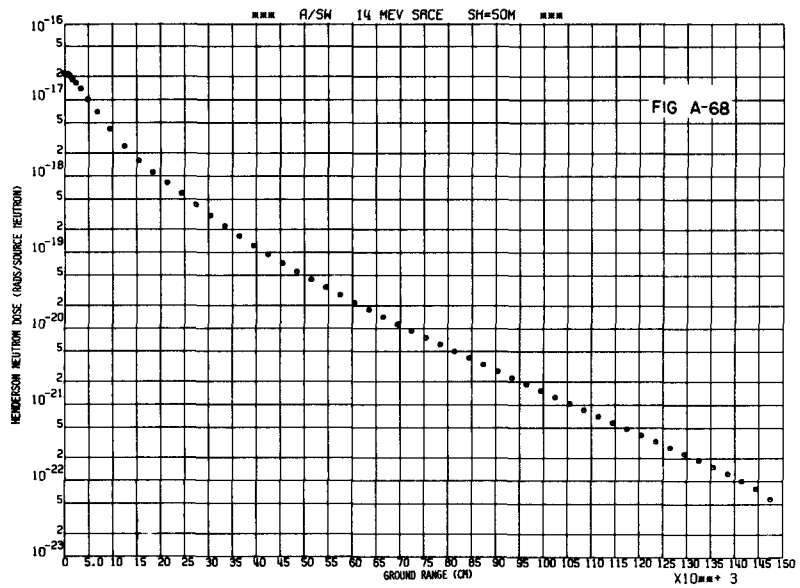
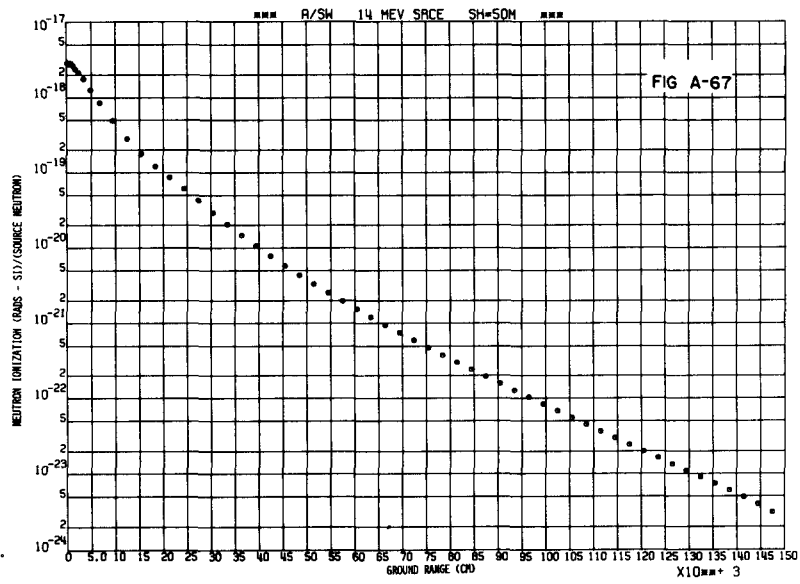


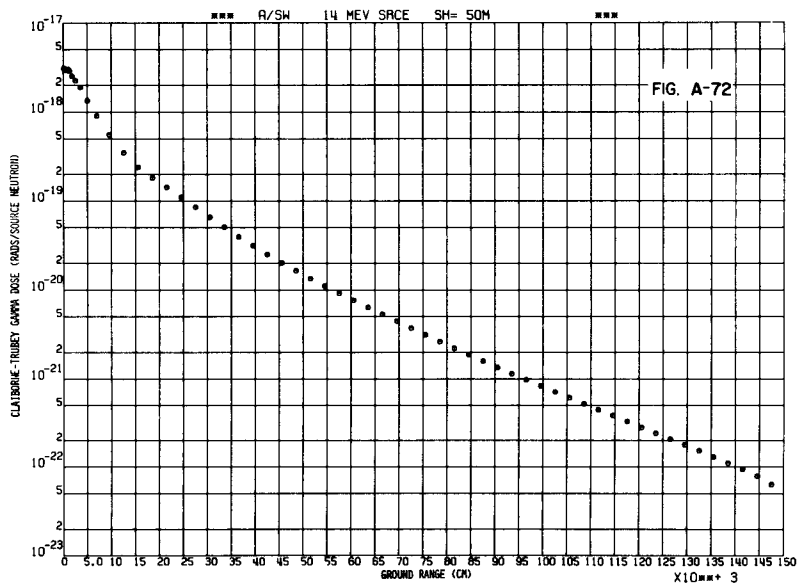
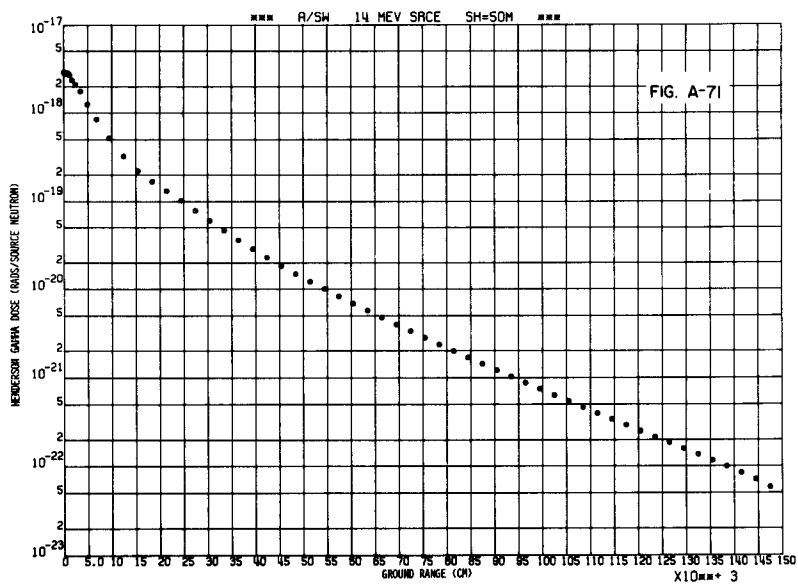
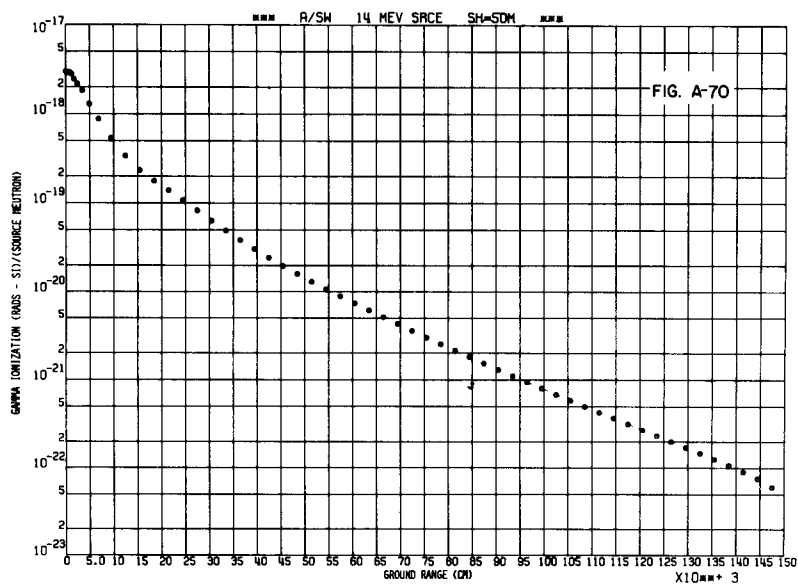














.

.



Internal Distribution

- | | | | |
|--------|----------------------|--------|--|
| 1-3. | L. S. Abbott | 41. | RSIC |
| 4-13. | D. E. Bartine | 42. | C. O. Slater |
| 14. | R. G. Alsmiller, Jr. | 43. | D. K. Trubey |
| 15. | R. L. Childs | 44. | C. R. Weisbin |
| 16. | C. E. Clifford | 45. | G. E. Whitesides |
| 17. | S. N. Cramer | 46. | A. Zucker |
| 18. | M. B. Emmett | 47. | P. F. Fox (consultant) |
| 19. | W. W. Engle, Jr. | 48. | W. W. Havens, Jr. (consultant) |
| 20. | H. Goldstein | 49. | A. F. Henry (consultant) |
| 21. | F. C. Maienschein | 50-51. | Central Research Library |
| 22-27. | F. R. Mynatt | 52. | ORNL Y-12 Technical Library,
Document Reference Section |
| 28. | E. M. Oblow | 53-54. | Laboratory Records Department |
| 29-38. | J. V. Pace, III | 55. | Laboratory Records ORNL RC |
| 39. | R. W. Peelle | 56. | ORNL Patent Office |
| 40. | F. G. Perey | | |

External Distribution

- 57. P. B. Hemmig, Division of Reactor Research and Development,
U. S. Energy Research & Development Administration,
Washington, D.C. 20545
- 58. Research and Technical Support Division, U. S. Energy Research
& Development Administration, Oak Ridge, Tennessee 37830
- 59-192. Given DNA Radiation Transport Distribution.
- 193-219. Technical Information Center, ORO.